Soil organic carbon stocks and quality in small-scale tropical, sub-humid and semi-arid watersheds under shrubland and dry deciduous forest in southwestern India

Severin-Luca Bellè, Jean Riotte, Muddu Sekhar, Laurent Ruiz, Marcus Schiedung, Samuel Abiven

Geoderma 409 (2022) 115606

Contents lists available at ScienceDirect

Geoderma

journal homepage: www.elsevier.com/locate/geoderma

Soil organic carbon stocks and quality in small-scale tropical, sub-humid and semi-arid watersheds under shrubland and dry deciduous forest in southwestern India

Severin-Luca Bellè [a], Jean Riotte [b,c], Muddu Sekhar [c,d], Laurent Ruiz [b,c,e], Marcus Schiedung [a], Samuel Abiven [a,f,g,*]

[a] Department of Geography, University of Zurich, Winterthurerstrasse 190, 8057 Zurich, Switzerland
[b] Géosciences Environnement Toulouse, Université Paul-Sabatier, IRD, CNRS, 14 Avenue E. Belin, 31400 Toulouse, France
[c] Indo-French Cell for Water Sciences, Indian Institute of Science, CV Raman Road, Bangalore, Karnataka 560012, India
[d] Department of Civil Engineering, Indian Institute of Science, CV Raman Road, Bangalore, Karnataka 560012, India
[e] UMR SAS, INRAE, Agrocampus Ouest 65 rue de St Brieuc, 35042 Rennes, France
[f] Laboratoire de Géologie, Département de Géosciences, CNRS – École normale supérieure, PSL Université, Institut Pierre Simon Laplace, Rue Lhomond 24, 75005 Paris, France
[g] CEREEP-Ecotron Ile De France, ENS, CNRS, PSL Université, Chemin de busseau 11, 77140 St-Pierre-lès-Nemours, France

ARTICLE INFO

Handling Editor: Budiman Minasny

Keywords:
Tropical soil
Soil organic carbon
Mid-infrared spectroscopy
Land-use transitions
Shrubland
Dry deciduous forest

ABSTRACT

Soil organic carbon is regulated by a dynamic interaction of vegetation inputs, organic matter degradation and stabilization processes in soils, and its redistribution in the landscape. Tropical ecosystems are highly important in terms of carbon stored in vegetation and soil, but many processes of the soil carbon cycle in the tropics are yet to be fully understood. Here, we studied soil organic carbon stocks and quality in small-scale tropical, sub-humid and semi-arid watersheds along a climate gradient in southwestern India with varying vegetation and geology to identify major drivers of soil organic carbon dynamics in three prevalent soil types (Lixisol, Vertisol and Ferralsol) under shrubland and dry deciduous forest. We used a combination of organic carbon analysis (total organic carbon content, ^{13}C, C:N), mid-infrared spectroscopy and soil property information (bulk density, texture, oxides, pH, cation-exchange capacity). Soil organic carbon stocks in these watersheds showed a substantial range from 58.2 to 169.4 Mg C ha^{-1} in the first 60 cm, and the differences depended on local- to watershed-scale variations in vegetation type and history, geology, soil physio-chemical (clay, oxides) and biological (bioturbation) properties. Considerable parts of the organic carbon stored in these soils was found below 30 cm (up to 40 %), stressing the importance of tropical subsoils. From our analysis of the soil organic carbon quality and literature data on paleoclimate and vegetation, we could identify land-use changes in these watersheds, from tropical moist evergreen forests, forest-savannah transitions and plantations to secondary regrowth forest over time. Our study provides new data and insights into the local-scale drivers of soil organic carbon quantity and quality of tropical, sub-humid and semi-arid watersheds under shrubland and dry deciduous forest with varying geology and soil types.

1. Introduction

Soils are a key component of the global carbon (C) cycle and are the major storage of biomass-derived organic carbon on Earth. Most recent estimates of the global soil organic carbon (SOC) pool account for 1325 to 1408 Pg C in the first metre and 2060 Pg C in the first two metres of soils (Batjes, 2016; Köchy et al., 2015). Tropical ecosystems are assumed the largest pool of terrestrial organic carbon in vegetation biomass due to high primary production, but also tropical soils are an important carbon pool (Beer et al., 2010). On a global scale, tropical ecosystems store 288 and 480 Pg C in soils under grassland/savannah and forest respectively (0–300 cm), and thus make up approximately one third of

* Corresponding author at: Laboratoire de Géologie, Département de Géosciences, CNRS – École normale supérieure, PSL Université, Institut Pierre Simon Laplace, Rue Lhomond 24, 75005 Paris, France.
E-mail address: abiven@biotite.ens.fr (S. Abiven).

https://doi.org/10.1016/j.geoderma.2021.115606
Received 9 July 2021; Received in revised form 15 November 2021; Accepted 17 November 2021
Available online 8 December 2021

organic carbon stored in soils (Carvalhais et al., 2014). Estimates of SOC stocks for tropical and subtropical forests can range from 94 to 143 Mg ha^{-1} (0–100 cm; (Duarte-Guardia et al., 2019)) to 239 Mg ha^{-1} (0–300 cm; (Carvalhais et al., 2014)). In addition, tropical grassland/savannah store between 99 and 104 Mg ha^{-1} (0–100 cm; (Duarte-Guardia et al., 2019)) and 151 Mg ha^{-1} (0–300 cm; (Carvalhais et al., 2014)).

Global ecosystem C estimations are dependent on uncertainties raising from spatial distribution of SOC data, from extrapolation to deeper soil horizons, from a lack of process understanding of SOC dynamics and from bulk density determination methodologies (Batjes, 2016; Dungait et al., 2012; Köchy et al., 2015). While tropical forests represent 45 % of the global forested land area (Poker and MacDicken, 2016), soils from tropical and subtropical forests combined account only for 11 % of all profiles in the World Soil Information Service (WoSIS) database of ISRIC. Around 18 % of the soil profiles in WoSIS are covered with tropical and subtropical grasslands, savannahs and shrublands (Batjes et al., 2020). In addition, the depth used for soil studies globally accounts for only 27 cm in average (Yost and Hartemink, 2020). However, subsoils (>20–30 cm) can store a large proportion of the global SOC (>50 %) and could be very sensitive to environmental perturbations such as land-use change or warming (Jobbágy and Jackson, 2000; Rumpel and Kögel-Knabner, 2011). Given these numbers, adding more data on SOC stocks and quality from tropical and subtropical regions, especially including subsoil horizons could be a valuable advancement of global SOC inventories.

For the Indian subcontinent, SOC stock estimations are ranging from 9.6 Pg C (0–30 cm) to 29.9 Pg C (0–150 cm) (Bhattacharyya et al., 2009; Gupta and Rao, 1994). Indian forest soils store around 4.1 Pg C (0–50 cm) and 6.8 Pg C (0–100 cm) (Chhabra et al., 2003), and SOC stocks estimations for the Western Ghats region in southwestern India are around 140 Mg ha^{-1} in the first metre (Dharumarajan et al., 2021). However, data coverage is scarce and soils from the Indian subcontinent account for only 199 profiles in the WoSIS (Batjes et al., 2020), evoking a need for more accurate field-data on SOC quantity and quality.

SOC stocks and quality show strong heterogeneity at the field and/or landscape level (Mishra and Riley, 2015), caused by varying land uses (transitions), vegetation histories, parent materials and soil types (Torn et al., 2009), but also by anthropogenic pressure on natural ecosystems (Grace et al., 2014). In fact, many tropical ecosystems are disturbed both in terms of vegetation and soil (Drake et al., 2019; Flores et al., 2020), which is also the case for the dry deciduous forest in southwestern India included in the present study (Mehta et al., 2008). However, our understanding of SOC quantity and quality in such disturbed tropical secondary (regrowth) forests, especially about dynamic transitions between land uses from savannah/grassland (pasture, shrubland) to forests and vice versa over decades, is still limited (Don et al., 2011; Marin-Spiotta et al., 2009; Oliveras and Malhi, 2016; Ratnam et al., 2011). The SOC quality, here referring to its compound-specific composition (i.e. aliphatic, aromatic or cellulose- and lignin-like compounds) and decomposition state, is a good proxy for vegetation and SOC dynamics. It can be assessed by mid-infrared spectroscopy that is a semi-quantitative, but highly efficient approach (Laub et al., 2020; Ramirez et al., 2021) in combination with organic carbon analyses (^{13}C, C:N).

In this study, we measured SOC stocks and its quality in 54 soil profiles of ten sites including prevalent soil types under tropical shrubland/open-mixed forest and dry deciduous forest in small-scale, sub-humid and semi-arid watersheds in southwestern India to address the following questions: 1) Do small-scale variations of climate, land uses, geology and soil types lead to clear differences in SOC stocks up to 60 cm? and 2) Can we explain the SOC stock and quality variations with differences in climate, vegetation (history), geology and soil properties. We selected six sites in the dry deciduous forest in Mule Hole watershed in the Bandipur National Park and Tiger Reserve, where always two sites corresponded to one of the three prevalent soil types of the region (Lixisol, Vertisol and Ferralsol) covering both prevalent gneiss and amphibolite bedrock. These three soil types cover 8.6 % (Vertisol), 11.2 % (Lixisol) and 19.3 % (Ferralsol) of the global land surface under forest, respectively (Poker and MacDicken, 2016; Zech et al., 2014). Three sites in the forest encompass a small landscape transect towards the streambed. In addition, we selected two sites under shrubland in the Maddur watershed close to the boarder of the Bandipur National Park and two sites under shrubland/open-mixed forest in the Bandipur National Park buffer zone in the drier southeastern part of the South Gundal basin corresponding to the forest-savannah transition. We used a combination of organic carbon analysis (SOC and ^{13}C), mid-infrared spectroscopy and basic soil and vegetation properties to answer the questions about the SOC stocks and quality in these tropical soils.

2. Material and methods

2.1. Study sites and watersheds

Fieldwork was carried out in the two small-scale tropical, sub-humid watersheds of Mule Hole (4.3 km^2) and Maddur (7.1 km^2), and in the semi-arid watershed of South Gundal (816 km^2), all draining first the Kabini river basin (7000 km^2) and subsequently the greater Cauvery river basin (87′900 km^2) on the Deccan plateau (Fig. 1 and Table 1; Robert et al., 2017). The three watersheds belong to the Kabini Critical Zone Observatory (Multiscale Tropical Catchments (M−TROPICS)) in Chamarajanagar district, southwestern Karnataka, India (Riotte et al., 2021; Sekhar et al., 2016).

The study sites and watersheds are located in a region with a distinct climatic gradient induced by the Western Ghats mountain range (Fig. 1 and Table 1), which forms an orographic barrier for precipitation, from the footslopes of the Ghats in the west towards the eastern portions of the Kabini river basin on the Deccan Plateau (Gunnell and Bourgeon, 1997). Precipitation shows a seasonal availability due to two monsoon seasons with dry spells in between (Maréchal et al., 2009; Riotte et al., 2021). In addition, due to natural variations in climate and subsequently vegetation in past and present, but also anthropogenic perturbations of the ecosystems, a transition between shrubland, savannah, degraded and pristine forest can be found in the research area (Caner et al., 2007).

The Mule Hole watershed, part of the Nugu watershed, is located in Bandipur National Park (11°43-44′ N, 76°26-27′ E) and is covered by secondary dry deciduous forest with varying composition depending on the underlying geology (see Table 1; Barbiéro et al., 2007; Riotte et al., 2014). Mule Hole forest originates from times before the independence of India (1947) and the creation of the National park (1973–1974), and was partially covered by former teak plantations. In recent years, *Lantana camara* (L.), an invasive shrub species from the American tropics, became a dominant understory plant. The geology consists mainly of Precambrian peninsular gneiss, but also scattered amphibolite (mainly containing quartz, oligoclase, sericite, biotite and chlorite in the primary mineral phase), covered by a saprolite layer varying in thickness, which itself is overlaid by a soil cover dominated by Vertisols in the valleys or footslopes, and (shallow) Ferralsols (chromic Luvisols) and Lixisols on hillslopes (Barbiéro et al., 2007; Braun et al., 2009). The terrain in Mule Hole is slightly undulating, with gentle slopes between 0 and 10° and elevation between 820 and 910 m.a.sl. (Fig. 1; Barbiéro et al., 2007). The pedoclimatic setting, parent rock and soil formation determine the occurrence of specific assemblages of clay minerals and secondary minerals (Fe-(oxyhdro)oxides, short-range order minerals). Kaolinite-dominated (shallow) Ferralsols and chromic Luvisol with intermingled goethite, residual quartz and Na-plagioclase and smectite-dominated Vertisols at the landscape bottom or the crest line are prevalent. Vertisols on gneiss further consist of kaolinite and interstratified kaolinite-smectite (Barbiéro et al., 2007; Riotte et al., 2014).

Maddur watershed, which is part of the Berambadi and South Gundal watersheds, lies to the eastern border of Bandipur National Park (11°47′ N, 76°33′ E) and is under partial cultivation in lower elevations and open-mixed shrubland/forest at hilltops (Violette et al., 2010b). The Precambrian peninsular gneiss is here covered by a thick saprolite layer

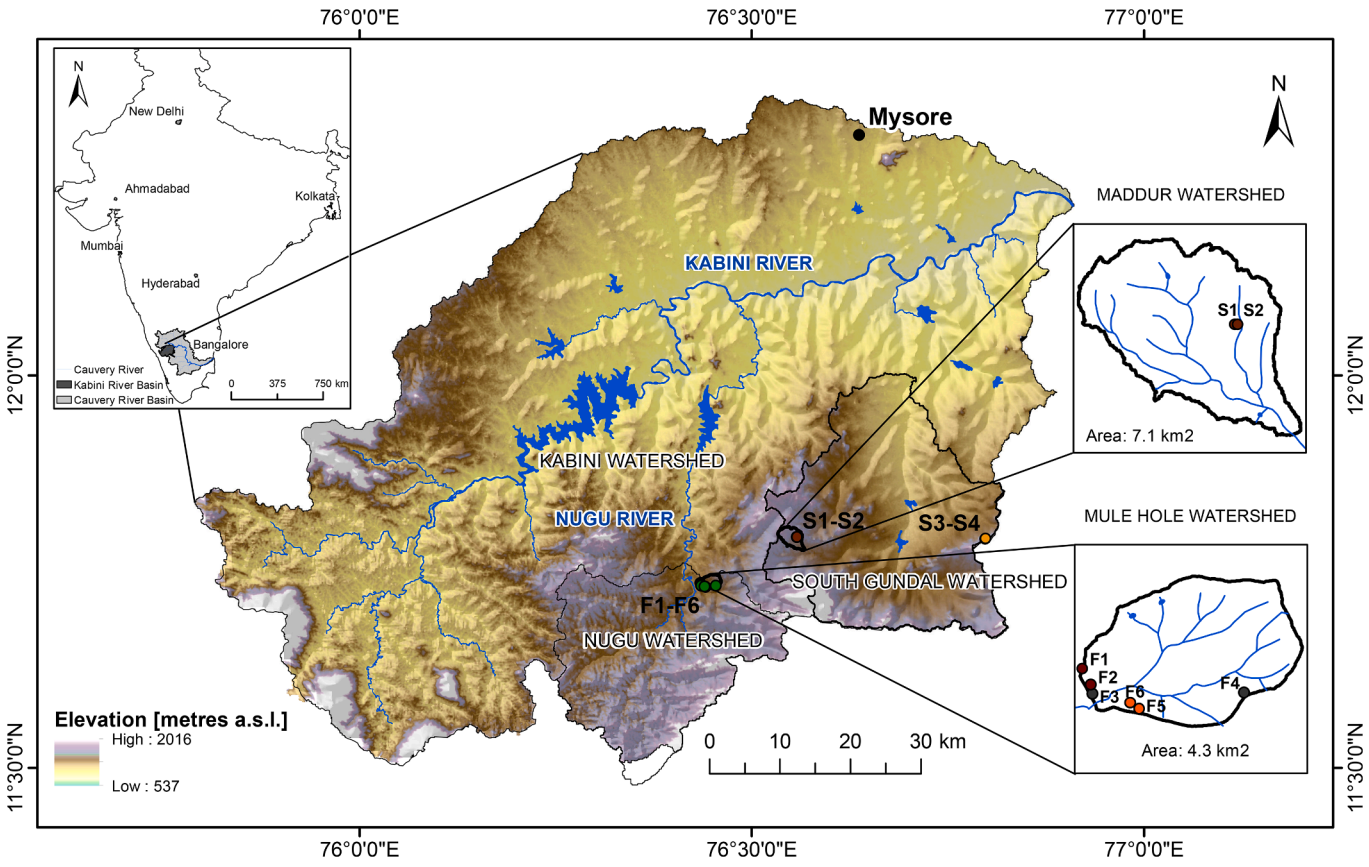

Fig. 1. Overview map(s) showing the greater Cauvery and Kabini river basin in southern India (top left) and the greater Kabini river basin that encompasses the Mule Hole (Nugu), Maddur and South Gundal watersheds (middle centre). Six sampling sites are located in the dry deciduous forest in Mule Hole watershed in Bandipur National Park (F1-F6: green circles), which is depicted in the panel on the bottom right (Lixisol: dark umber, Vertisol: dark grey and Ferralsol: fire red). Two sampling sites are located in Maddur watershed under shrubland (S1-S2: brown circles; see panel top right) and two sampling sites in the Bandipur National Park buffer zone that is part of the South Gundal watershed under open-mixed shrubland/forest (S3-S4: orange circles). (For interpretation of the references to colour in this figure legend, the reader is referred to the web version of this article.)

that forms the basis for the Ferralsols and Lixisols of various thickness (Table 1).

The Bandipur National Park buffer zone, partially covering the semi-arid, southeastern parts of the South Gundal watershed (11°47′ N, 76°47′ E), is covered by open-mixed shrubland/forest. The simultaneous occurrence of a discontinuous tree canopy and partially continuous C_4-grass cover could be read that the system represents a tropical savannah (Ratnam et al., 2011). However, since the area is managed by the national park, we classified it as open-mixed shrubland/forest instead of savannah. The main difference in vegetation between the Bandipur National Park buffer zone and the Mule Hole forest in Bandipur National Park is the tree canopy, which is much denser in Mule Hole despite of the presence of continuous C_4-grass understory. The occurring Ferralsols and Lixisols are generally shallower compared to the soils in the other watersheds, and the saprolite consisting of weathered Precambrian peninsular gneiss can already start in 20–30 cm depth in many cases (Table 1).

2.2. Field sampling design

We included two sites (S1-S2) close to hilltops (3-8° slope) near the spring in Maddur watershed close to the forest border and under (open) shrubland, still showing traces of cattle grazing (Fig. 1 and Table 1). We selected two sites in the Bandipur National Park buffer zone in the semi-arid region of the South Gundal basin. The two sites (S3-S4; Fig. 1 and Table 1) are along a gentle hillslope (8-12°). We sampled six sites in Mule Hole watershed in Bandipur National Park under dry deciduous forest (Fig. 1); however, we did not sample in the pristine forest itself. From these six sites, always two sites correspond to one of the three predominant soil types (Lixisol (F1-F2), Vertisol (F3-F4) and Ferralsol (F5-F6) respectively). This allowed us to integrate the variety of soil genesis of the landscape within specific soil types, i.e. including a Vertisol developed on Precambrian gneiss (F3) and a Vertisol developed on mafic rocks such as amphibolite (F4), but also a shallow Ferralsol on gneiss (F5) and a Ferralsol on gneiss (F6; Fig. 1 and Table 1). The sites F1-F3 formed a topographic sequence from hillslope positions (F1-F2) to the streambed (F3). Slopes ranged from 0 to 5° (F3-F4), 1-5° (F5-F6) and 6-10° (F1-F2).

Each site consisted of a 25 × 25 m plot, in which we excavated five soil pits by hand (0–60 cm); resulting in 54 soil profiles (nine pits were sampled in site S1). The five pits were arranged so that there was a main characterisation pit in the centre and four pits towards the four edges of the plot (defined by coordinates taken for all four edges and the five pits) in order to integrate the spatial variability, in particular of soil organic carbon. We sampled the soil profile in each of the pits in four depth increments (0–15, 15–30, 30–45 and 45–60 cm) with a soil corer (12 cm length, 5 cm diameter) positioned horizontally and a hammering head. The core was taken in the centre of the 15 cm increment (therefore leaving a 3–4 cm gap between each increment). In specific cases, we could take samples up to 2 m (Table 2). We took three cores per depth increment and pit, which were subsequently composited in the field. Per site, this makes a maximum of 20 samples (except for site S1: 36 samples); however, not every pit could be sampled up to 60 cm with a soil corer due to presence of saprolite and high stone contents. In some cases, we could take shovel samples instead. The pit core samples were pre-sieved to < 8 mm for homogenisation, sample mass reduction for

Table 1
Basic information of the ten sites in the tropical, sub-humid and semi-arid watersheds of Maddur, South Gundal and Mule Hole in southwestern Karnataka, India.

Site	Coordinates	Watershed	MAT [°C] [1]	MAP [mm yr^{-1}] [2]	Land use	Vegetation (dominant species)[3]	Geology[4]	Soil type (WRB)
S1	11°47′37′′ N; 76°33′27′′ E	Maddur	23	830	Shrubland	Scrubs, patches of deciduous forest	Peninsular Precambrian gneiss	epileptic Lixisol
S2	11°47′38′′ N; 76°33′28′′ E	Maddur	23	830	Shrubland	Scrubs, patches of deciduous forest	Peninsular Precambrian gneiss	epileptic Lixisol
S3	11°47′29′′ N; 76°47′55′′ E	South Gundal	23.6	630	Open-mixed shrubland/forest	*Euphorbia lactea, Azadirachta indica, Senna siamea, Heteropogon contortus*	Peninsular Precambrian gneiss	epileptic skeletic Lixisol
S4	11°47′31′′ N; 76°47′54′′ E	South Gundal	23.6	630	Open-mixed shrubland/forest	*Euphorbia lactea, Azadirachta indica, Senna siamea, Heteropogon contortus*	Peninsular Precambrian gneiss	epileptic skeletic Lixisol
F1	11°44′06′′ N; 76°26′03′′ E	Mule Hole	22	1170	Dry deciduous forest	ATT facies[a], *Themeda triandra, Lantana camara*	Peninsular Precambrian gneiss	xanthic ferralic Lixisol (clayic)
F2	11°43′59′′ N; 76°26′07′′ E	Mule Hole	22	1170	Dry deciduous forest	ATT facies, *Themeda triandra, Lantana camara*	Peninsular Precambrian gneiss	ferric Lixisol
F3	11°43′55′′ N; 76°26′08′′ E	Mule Hole	22	1170	Dry deciduous forest	ATT facies, *Themeda triandra, Ceriscoides turgida, Lantana camara*	Peninsular Precambrian gneiss	pellic calcic Vertisol
F4	11°43′55′′ N; 76°27′15′′ E	Mule Hole	22	1170	Dry deciduous forest	ATT facies, *Themeda triandra, Ceriscoides turgida, Lantana camara*	Amphibolite	pellic Vertisol ferric
F5	11°43′48′′ N; 76°26′29′′ E	Mule Hole	22	1170	Dry deciduous forest	ATT facies, Shorea facies (*Shorea roburghii and Lagerstroemia microcarpa*), *Themeda triandra, Lantana camara*	Peninsular Precambrian gneiss	lixic Ferralsol
F6	11°43′51′′ N; 76°26′25′′ E	Mule Hole	22	1170	Dry deciduous forest	ATT facies, *Themeda triandra, Lantana camara*	Peninsular Precambrian gneiss	lixic Ferralsol

[1,2] Data from Violette et al. (2010a, 2010b) and Riotte et al. (2021).
[3] Data from Barbiéro et al. (2007), Riotte et al. (2014, 2021) and field observations.
[4] Data fromBraun et al. (2009).
[a] ATT facies: *Anogeissus latifolia, Tectona grandis, Terminalia crenulata.*

transportation and air-dried.

Standardized bulk density (BD) cores (100 cm^3) were sampled for each depth in each pit (162 BD cores for 189 pit core samples for which the stone content was suitable for sampling). BD cores were weighed in the field, dried at 105° C for 24 h, subsequently weighed to determine field moisture content, and sieved to < 2 mm to determine the mass of root and stone fragments.

2.3. Sample preparation

All pit core samples were dried at 40° C for 48 h and subsequently sieved to < 2 mm. For the analysis of total carbon (TC), total organic carbon (TOC), $\delta^{13}C$, total nitrogen (TN), pH, diffuse reflectance infrared Fourier-transformed spectroscopy (DRIFT) and X-ray fluorescence (XRF), samples were milled using a horizontal mill (2–5 min, 30 turns/s). For the analysis of pH, electrical conductivity (EC), cation-exchange capacity (CEC), texture and XRF, a composite sample per depth increment and site was produced from the pit core samples.

2.4. Sample laboratory analysis

The pH and EC were measured on composited samples (1 g of milled sample from each depth increment and pit per site were mixed to a composite of 5 g in a 50 ml centrifuge tube) with a 914 pH/Conductometer (Methrom, Herisau, Switzerland) according to Carter and Gregorich (2008). Briefly, the soil mass (5 g) was mixed with 0.01 M $CaCl_2$ in a ratio of 1:2.5, shaken by hand until complete suspension and put to settle for one hour before measurement in the suspension.

Total elemental composition was measured with an energy dispersive X-ray fluorescence spectrometer (SPECTRO XEPOS, SPECTRO Analytical Instruments GmbH, Kleve, Germany) on milled, composited samples. An internal soil standard was used for calibration and reference (NCS DC 73319). Total elemental concentrations were then converted to weight percent of oxides. The sum of major oxides (SiO_2, Al_2O_3, Fe_2O_3, K_2O, Na_2O, CaO, P_2O_5, MgO, MnO, TiO_2) plus the organic matter (calculated as the TOC (%, see Table 2) multiplied by 1.72) and $CaCO_3$ (calculated as the TIC (%; TC-TOC, see Table 2) multiplied by (100/12.01)) accounted for 81–99 % of dry soil mass (mean = 88 %). The remaining difference could be attributed to weight percentage of other trace oxides and residual water (Loss on ignition (LOI) represented 9.6–10.5 % for the Ferralsol and 8.6–9.9 % for the Vertisol in previous studies from Mule Hole).

Chemical compounds of SOC were characterised by diffuse reflectance infrared Fourier-transformed spectroscopy (DRIFT) analysis (TENSOR 27 spectrophotometer, Bruker, Switzerland). Spectra were obtained on all samples in the wavelengths between 4000 and 400 cm^{-1} (64 scans on each sample with a resolution of 4 cm^{-1}). Prior to measurements, atmospheric variations were integrated by running a potassium bromide background calibration. Acquired spectra were analysed with R Studio 1.3.1093 (R Core Team, 2020) after baseline correction. Maximum absorbance were selected for specific peaks in the wavelength ranges of 2930–2850 cm^{-1} (aliphatic compounds), 1660–1600 cm^{-1} (aromatic compounds), 1510–1500 cm^{-1} (lignin), 1260–1210 cm^{-1} (cellulose) and 893–852 cm^{-1} (aromatic compounds) according to ranges identified previously (e.g. Chatterjee et al., 2012; Laub et al., 2020; Yeasmin et al., 2017). Two ratios of aliphatic/aromatic (using the aromatic peaks at 1630 and 880 cm^{-1} respectively) and one of cellulose/lignin were calculated to assess qualitatively SOC dynamics with depth.

Soil texture was measured according to a protocol (NF X31.107), which follows the sedimentation and pipette method for particle size determination after removal of organic matter with H_2O_2 (ISO 11277). The effective CEC and exchangeable cations were measured following the standard protocol ISO 23470:2018 in a hexamminecobalt trichloride

Table 2

Bulk density (BD), total carbon (TC, TC_δ^{13}C), total organic carbon (TOC, TOC_ δ^{13}C), total nitrogen (TN), C:N ratio (CN), pH, electrical conductivity (EC), cation-exchange capacity (CEC), texture (clay (<2 μm), silt (2–50 μm), sand (50 μm – 2 mm)), weight percent of iron (Fe_2O_3), aluminium (Al_2O_3) and silicon (SiO_2) oxides for each depth increment and site. Values are means of field replicates per site (standard error in parentheses) except if indicated otherwise in column "n". n.d. = not determined.

Site	Depth	n[a]	BD	TC	TC_δ^{13}C	TOC	TOC_δ^{13}C	TN	C:N	pH	EC	CEC	Clay	Silt	Sand	Fe	Al	Si
	[cm]		[g cm^{-3}]	[%]	[‰]	[%]	[‰]	[%]	[-]	[-]	[μS cm^{-1}]	[meq/100g]	[%]	[%]	[%]	[%]	[%]	[%]
S1	0–15	9	1.23 (0.04)	1.47 (0.08)	−22.73 (0.33)	1.21 (0.05)	−23.42 (0.38)	0.11 (0.01)	11.40 (0.55)	5.6	2.2	8.9	16.9	18.8	64.3	4	18	59
	15–30	7	1.13 (0.07)	1.13 (0.06)	−22.94 (0.33)	1.06 (0.06)	−23.47 (0.40)	0.09 (0.01)	12.11 (0.38)	5.5	1.7	8.4	20.2	18.8	61.0	3	16	61
	30–45	4	1.02 (0.11)	0.77 (0.11)	−23.50 (0.43)	0.71 (0.08)	−24.20 (0.39)	0.07 (0.01)	10.15 (0.76)	5.2	1.6	n.d.	n.d.	n.d.	n.d.	n.d.	n.d.	n.d.
	45–60	3	1.25 (0.04)	0.63 (0.19)	−24.55 (0.35)	0.55 (0.14)	−24.89 (0.39)	0.05 (0.01)	9.93 (0.52)	5.3	2.1	n.d.	n.d.	n.d.	n.d.	n.d.	n.d.	n.d.
S2	0–15	5	1.33 (0.05)	1.68 (0.32)	−25.21 (0.51)	1.00 (0.09)	−26.32 (0.58)	0.12 (0.02)	8.86 (0.93)	5.6	2.2	9.6	18.1	18.8	63.2	3	17	59
	15–30	5	1.18 (0.04)	1.35 (0.25)	−25.03 (0.64)	0.85 (0.08)	−26.45 (0.63)	0.11 (0.02)	9.00 (1.18)	5.9	2.0	10.3	22.3	19.4	58.3	4	17	59
	30–45	3	1.18 (0.00)	1.37 (0.29)	−25.45 (0.83)	0.88 (0.10)	−26.98 (0.86)	0.11 (0.02)	8.38 (0.81)	6.8	1.9	15.0	26.9	20.1	53.0	4	18	55
S3	0–15	5	0.98 (0.06)	1.89 (0.08)	−25.44 (0.41)	1.66 (0.16)	−25.89 (0.85)	0.13 (0.02)	16.32 (5.96)	6.5	1.9	12.7	17.0	23.0	60.0	8	17	51
	15–30	3	0.85 (0.12)	1.18 (0.03)	−20.15 (0.81)	1.22 (0.02)	−21.25 (0.35)	0.11 (0.01)	11.60 (1.51)	5.9	2.1	8.1	18.8	24.4	56.8	8	18	53
	30–45	3	1.04 (0.13)	0.94 (0.16)	−20.26 (0.86)	0.92 (0.17)	−21.37 (0.18)	0.09 (0.00)	9.76 (1.83)	6.0	2.2	13.7	20.7	23.1	56.2	10	19	47
	45–60	2	1.00 (0.21)	0.73 (0.14)	−21.17 (0.21)	0.88 (0.22)	−22.53 (0.07)	0.07 (0.00)	12.48 (3.30)	6.1	2.1	n.d.	n.d.	n.d.	n.d.	n.d.	n.d.	n.d.
S4[b]	0–15	5	0.89 (0.09)	1.89 (0.26)	−23.04 (0.92)	1.69 (0.13)	−23.13 (1.06)	0.09 (0.02)	22.78 (4.94)	6.1	2.2	10.5	16.2	22.6	61.2	7	17	54
	15–30	5	1.25 (0.09)	1.08 (0.10)	−19.27 (0.17)	1.05 (0.05)	−18.91 (0.26)	0.12 (0.02)	9.27 (1.19)	5.8	2.1	9.0	16.4	21.2	62.4	8	18	53
	30–45	3	0.89 (0.07)	1.02 (0.14)	−18.76 (0.33)	0.96 (0.15)	−18.93 (0.27)	0.08 (0.01)	11.63 (0.86)	5.8	2.1	11.0	17.6	21.6	60.8	8	17	51
	45–60	3	0.98 (0.00)	0.96 (0.18)	−19.12 (0.36)	0.84 (0.16)	−19.77 (0.34)	0.08 (0.00)	9.99 (1.26)	5.7	2.2	10.8	21.3	21.5	57.2	6	19	55
F1	0–15	5	1.54 (0.02)	2.03 (0.18)	−26.56 (0.34)	1.54 (0.17)	−27.09 (0.28)	0.13 (0.01)	11.81 (0.83)	5.9	2.2	10.9	11.9	23.8	64.3	3	11	64
	15–30	5	1.43 (0.04)	0.79 (0.06)	−23.24 (0.36)	0.83 (0.06)	−24.07 (0.24)	0.07 (0.00)	12.78 (0.72)	5.1	2.2	6.2	15.4	20.5	64.1	4	14	64
	30–45	5	1.33 (0.10)	0.55 (0.04)	−23.16 (0.29)	0.60 (0.05)	−23.42 (0.43)	0.05 (0.00)	11.18 (0.90)	4.9	2.1	8.4	19.4	20.7	59.9	5	13	65
	45–60	5	1.17 (0.10)	0.46 (0.03)	−22.74 (0.50)	0.46 (0.03)	−23.00 (0.35)	0.05 (0.00)	8.92 (0.35)	4.8	2.1	10.9	32.5	17.8	49.8	6	18	56
F2	0–15	5	1.42 (0.03)	3.29 (0.19)	−27.24 (0.31)	1.82 (0.26)	−28.07 (0.27)	0.20 (0.01)	8.81 (0.84)	5.9	2.2	19.2	20.5	26.5	53.0	4	14	59
	15–30	5	1.44 (0.02)	1.68 (0.14)	−24.96 (0.10)	1.28 (0.12)	−26.07 (0.36)	0.13 (0.01)	10.26 (0.98)	5.7	2.2	13.7	21.0	24.1	54.9	5	15	57
	30–45	5	1.35 (0.11)	1.05 (0.08)	−24.19 (0.19)	1.03 (0.07)	−24.81 (0.34)	0.08 (0.00)	12.40 (0.81)	5.2	2.2	10.0	22.4	20.9	56.6	7	15	57
	45–60	5	1.00 (0.16)	0.75 (0.04)	−22.95 (0.23)	0.73 (0.02)	−23.36 (0.48)	0.07 (0.00)	11.14 (0.27)	5.1	2.1	10.7	32.0	19.2	48.8	10	19	49
F3[c,d]	0–15	5	1.37 (0.02)	4.24 (0.23)	−27.47 (0.20)	2.38 (0.21)	−28.93 (0.20)	0.27 (0.01)	9.05 (0.88)	6.0	2.1	36.2	29.4	35.7	34.9	4	12	55
	15–30	5	1.36 (0.03)	1.92 (0.10)	−25.81 (0.21)	1.51 (0.10)	−26.88 (0.26)	0.15 (0.01)	10.47 (0.61)	5.7	2.1	32.1	36.1	31.1	32.8	5	14	56
	30–45	5	1.32 (0.03)	1.39 (0.20)	−21.77 (1.53)	1.15 (0.12)	−25.35 (0.41)	0.08 (0.01)	14.23 (1.33)	6.7	2.0	37.1	44.2	30.5	25.3	5	14	52
	45–60	5	1.39 (0.03)	1.44 (0.32)	−19.71 (1.74)	0.75 (0.10)	−24.31 (0.43)	0.07 (0.00)	10.90 (1.73)	6.9	< 1	36.3	46.2	29.9	23.9	5	13	54
	60–80	1	n.d.	1.12	−23.42	1.09	−23.66	0.07	16.76	5.3	1.9	14.4	21.3	23.5	55.2	4	13	66
	80–100	1	n.d.	0.98	−25.44	0.95	−25.97	0.07	12.77	5.3	1.7	13.2	21.0	25.4	53.7	4	13	65
	100–150	1	n.d.	0.83	−24.99	0.82	−25.46	0.06	14.41	5.3	1.8	15.8	21.9	27.2	50.9	4	14	66
	150–200	1	n.d.	0.84	−24.96	0.87	−24.87	0.05	17.79	5.5	2.1	13.8	23.0	24.5	52.5	4	14	63
F4	0–15	5	1.29 (0.05)	4.21 (0.11)	−25.25 (0.32)	3.39 (0.42)	−25.71 (0.38)	0.28 (0.01)	12.17 (1.27)	5.7	2.1	38.0	37.1	35.9	27.0	10	14	44
	15–30	5	1.13 (0.12)	2.63 (0.08)	−24.22 (0.38)	2.54 (0.26)	−25.23 (0.50)	0.19 (0.01)	13.57 (1.54)	5.4	2.1	31.0	41.6	28.4	30.0	12	15	43
	30–45	5	0.96 (0.17)	1.88 (0.06)	−23.74 (0.32)	2.09 (0.08)	−23.32 (0.26)	0.15 (0.00)	13.93 (0.30)	5.2	< 1	28.8	47.2	25.4	27.5	12	17	42
	45–60	4	1.28 (0.05)	1.58 (0.09)	−23.21 (0.39)	1.69 (0.08)	−22.12 (0.20)	0.12 (0.01)	14.74 (0.60)	5.2	2.2	26.8	45.1	23.8	31.1	14	18	40
F5	0–15	5	1.54 (0.03)	2.01 (0.13)	−25.99 (0.11)	1.75 (0.10)	−26.47 (0.18)	0.15 (0.01)	11.67 (0.59)	5.5	2.2	10.5	16.2	31.8	51.9	4	14	59
	15–30	5	1.45 (0.08)	1.14 (0.10)	−24.09 (0.11)	1.08 (0.10)	−24.37 (0.13)	0.08 (0.01)	12.72 (0.57)	5.4	2.1	9.0	17.2	32.5	50.3	5	16	59
	30–45	5	1.30 (0.04)	0.79 (0.08)	−24.36 (0.48)	0.76 (0.07)	−24.11 (0.22)	0.07 (0.00)	11.61 (0.54)	5.3	1.7	8.1	18.7	28.6	52.7	7	18	57
	45–60	4	0.66 (0.01)	0.57 (0.01)	−23.96 (0.56)	0.56 (0.04)	−23.73 (0.27)	0.06 (0.00)	9.97 (0.64)	5.3	1.9	7.8	25.8	24.2	50.0	9	20	50
F6	0–15	5	1.40 (0.10)	3.15 (0.14)	−25.74 (0.36)	2.44 (0.08)	−26.83 (0.40)	0.20 (0.01)	12.28 (0.58)	5.5	1.2	17.5	23.6	30.0	46.4	6	14	52
	15–30	5	1.31 (0.17)	2.04 (0.07)	−24.26 (0.16)	1.82 (0.06)	−24.57 (0.29)	0.14 (0.00)	13.08 (0.49)	5.2	1.8	12.8	28.3	29.5	42.2	6	16	53
	30–45	5	1.19 (0.14)	1.41 (0.09)	−24.15 (0.40)	1.36 (0.07)	−24.39 (0.48)	0.11 (0.01)	12.87 (0.57)	5.1	1.9	12.5	30.7	25.6	43.7	9	19	49
	45–60	5	1.01 (0.13)	1.24 (0.15)	−24.01 (0.27)	1.14 (0.10)	−24.21 (0.17)	0.09 (0.01)	12.87 (0.69)	5.2	1.6	12.5	31.8	25.8	42.5	11	19	45
	60–80	1	n.d.	0.93	−23.27	0.89	−23.30	0.07	12.22	5.5	1.1	14.4	41.6	22.9	35.5	12	21	42
	80–100	1	n.d.	0.66	−22.76	0.61	−22.61	0.05	12.00	5.4	< 1	13.1	40.0	19.9	40.1	11	22	43

[a] n applies to BD, TC, TC_^{13}C, TOC, TOC_^{13}C, TN and CN ratio (= average values for each depth increment and pit per site (standard error in parentheses)). The pH, EC, CEC, texture, Fe, Al, Si are single measurements on composite samples of each depth increment per site (composite of all pits per depth increment if in three (or more) out of the five pits the respective depth increment was sampled).

[b] In site S4, black spear grass (*Heteropogon contortus*), a tropical perennial C_4-grass is abundant (TC = 40.81 ± 10.4 %, δ^{13}C: -13.03 ± 0.23 ‰). This grass species can also be found in site S1-S3.

[c] In site F3, calcite (secondary carbonates) is present between 30-60 cm (TC = 12.24 ± 0.03 %, δ^{13}C = -5.68 ± 0.92 ‰).

[d] Deep samples (60-200 cm) were taken adjacent to the soil profiles of site F3 at an opening of the river bank.

solution. The TN content of all milled samples was determined by dry combustion according to the DUMAS method following the standard protocol ISO 13878:1998.

The TOC content of all samples was determined following carbonates removal by the acid fumigation protocol described by Walthert et al. (2010). Prior to the fumigation, we determined the TC and $\delta^{13}C$ of samples to evaluate carbonate contents in the samples. Most samples contained inorganic C, especially those were secondary carbonates were present in soils (in particular F3; see Table 2). Briefly, 12–25 mg of milled sample (depending on expected C contents) was weighed in silver capsules and placed in the wells of a titer plate. Then, 50 μL of 1 % HCl were added to each capsule and exposed to 37 % HCl vapour for 8 h. Next, the samples were dried in a vaccumized desiccator for 24 h and subsequently in a vacuum oven at 35-40° C for three days (Walthert et al., 2010). The TC, TOC and $\delta^{13}C$ (of both TC and TOC) of all samples were measured on milled samples using cavity ring-down spectroscopy with a dry combustion module, relative to the international Vienna Pee Dee Belemnite (VPDB) standard (CRDS Picarro, Inc. 2020).

2.4.1. Soil organic carbon stock calculation

The SOC stock for each depth increment and pit in all sites was calculated according to the equations (M2) proposed by Poeplau et al. (2017):

$$BD_{finesoil} = \frac{m_{sample} - m_{rockfragments} - m_{rootfragments}}{V_{sample} - \frac{m_{rockfragments}}{\rho_{rockfragments}} - \frac{m_{rootfragments}}{\rho_{rootfragments}}} \quad (1)$$

where $BD_{fine\ soil}$ is the fine soil bulk density of each depth increment per pit (g cm^{-3}), m_{sample} is the total dry soil sample mass (g), $m_{rock\ fragments}$ and $m_{root\ fragments}$ are the masses of stones and roots > 2 mm (g), V_{sample} is the volume of the core sample (standardized 100 cm^3 corer), and $\rho_{rock\ fragments}$ and $\rho_{root\ fragments}$ are the density of rocks (2.6 g cm^{-3}) and assumed density of roots (1.0 g cm^{-3}) respectively. Using the $BD_{fine\ soil}$, the SOC stock per depth increment can be calculated as follow:

$$SOC_{stock} = TOC_{finesoil} \times BD_{finesoil} \times depth \times 100 \quad (2)$$

where SOC_{stock} is the soil organic carbon stock of each depth increment per pit (Mg ha^{-1}), $TOC_{fine\ soil}$ is the total organic carbon content of the corresponding fine soil sample (g g^{-1}), $BD_{fine\ soil}$ is the fine soil bulk density of each depth increment per pit (g cm^{-3}), depth is the 15 cm depth increment (cm) and the factor 100 is the unit conversion from g cm^{-2} to Mg ha^{-1}. Subsequently, cumulated SOC stocks were calculated for each depth increment and pit through the addition of individual SOC stocks per depth increments on each other and then averaged for each depth increment per site (for number of replication per depth see Table 2). When no BD data was available for a given depth in a pit due to high stone contents in deeper soil horizons, we used either the average BD for the same depth in the other pits of the site, or the BD from the depth above in the same pit.

2.5. Statistical analysis

We performed a linear regression analysis on the cumulated SOC stocks between sites for each depth increment independently (0–15, 15–30, 30–45 and 45–60 cm). Levene's test was used to check the assumption of homogeneity of variance (centre = mean). A one-way analysis of variance (ANOVA) was used on the cumulated SOC stocks with the site as independent variable. We ran the Shapiro-Wilk test on the ANOVA residuals to check for the assumption of normality and performed a Fisher's least significant difference (LSD) post-hoc test (alpha = 0.05, p.adj = bonferroni). We used simple correlation tests between SOC stocks, TOC and TN contents with essential soil properties (pH, EC, CEC, clay, silt, sand; Fe, Al, Si, K, Na, Ca, P, Mg, Mn, Ti weight percent of oxides), applying a Pearson Correlation (r) analysis, to assess major drivers of SOC storage and dynamics. All statistical analyses were completed using R Studio 1.3.1093 (R Core Team, 2020). Values are reported as means with one standard error of the mean.

3. Results and discussion

3.1. Soil organic carbon stocks under different vegetation and land-uses

SOC stock (and quality) differences between soils under open-mixed shrubland/forest and dry deciduous forest can be explained by the present-day vegetation density, composition and productivity that is higher in forests, which determines the quantity and composition of plant litter inputs (Beer et al., 2010; Carvalhais et al., 2014; Proulx et al., 2015), and the vegetation history of the studied watersheds.

SOC stocks were generally higher in forested sites of the sub-humid watershed (Mule Hole: F1-F6) compared to shrubland sites in the semi-arid watershed (South Gundal: S3-S4); however, no differences were observed between the shrubland sites in the sub-humid watershed of Maddur (S1-S2) and the semi-arid watershed of South Gundal (S3-S4; Fig. 2). The differences in precipitation intensity and repartition between shrubland and forest sites (Fig. 1 and Table 1) are causing differences in net primary production; consequently, the balance between plant C inputs and decomposition of SOC are to a certain degree moisture-limited. Furthermore, precipitation functions as a driver of weathering processes in soils (production of oxides, vertical transport of clay and silt or reduction in pH), which can lead to reduced SOC mineralisation. However, since climate (precipitation gradient) varies only slightly, it may be less relevant for the SOC storage at the local- to watershed-scale considered (González-Domínguez et al., 2019; Hombegowda et al., 2016).

The cumulated SOC stocks in 0–60 cm varied between 58.2 ± 9.0 (S1) to 66.8 ± 3.2 Mg ha^{-1} (S3) in the four Lixisols under open-mixed shrubland/forest (S1-S4; Fig. 2). These stocks were in the same range than modelled SOC stocks of 62–80 Mg ha^{-1} for the first metre under tropical mixed shrubland/grassland (Nayak et al., 2020). They were lower compared to global estimates for tropical grassland (100.9 Mg ha^{-1} for 0–100 cm; (Duarte-Guardia et al., 2019)) or tropical grassland/savannah ecosystems (108–218 Mg ha^{-1} for 0–300 cm; (Carvalhais et al., 2014)), but for different depth intervals. Differences here could be related to definitions of land-use transitions between shrubland, grassland and the forest-savannah frontier (Oliveras and Malhi, 2016; Ratnam et al., 2011) or methodologies of SOC stock calculations, bulk density correction and soil depth considered. Soils with high stone contents (>30 vol%) can lead to substantial overestimations of SOC stocks if bulk densities are not corrected for root and stone contents accordingly (Poeplau et al., 2017). The soils in the present study covered a deeply weathered saprolite layer with stone contents of up to 50 %, which we corrected in our SOC stock calculation.

The Lixisols under forest contained between 73.2 ± 4.3 to 98.2 ± 9.1 Mg SOC ha^{-1} in 0–60 cm (F1-F2), and these were not significantly different from the Lixisols under open-mixed shrubland/forest (Fig. 2; $p > 0.05$). In case of the upslope forest site (F1), the stocks were lower compared to all other forest soils except the shallow Ferralsol on gneiss (F5), and in case of the mid-slope forest site (F2) it was lower only compared to the elevated Vertisol on amphibolite (F4; $p < 0.05$). The shallow Ferralsol (F5: 84.8 ± 6.1 Mg ha^{-1}) contained comparable SOC to the Lixisols under forest, but showed significantly lower ($p < 0.05$) stocks than the Ferralsol on gneiss (F6) and the Vertisol on amphibolite (F4). The Vertisol on gneiss close to the streambed (F3: 117.6 ± 7.2 Mg ha^{-1}) showed higher SOC stocks compared to the other forest soils, but comparable stocks to the Ferralsol on gneiss (F6: 129.4 ± 9.6 Mg ha^{-1}; $p > 0.05$) and much lower stocks than the Vertisol on amphibolite (F4: 169.4 ± 5.9 Mg ha^{-1}; $p < 0.05$) in the first 60 cm (Fig. 2).

The average SOC stock in 0–60 cm for all forest soils in this study (111.0 ± 6.5 Mg ha^{-1}) was well in line with estimated stocks based on digital soil mapping using remote sensing data for the Western Ghats ecoregion (107.1 ± 47.0 Mg ha^{-1} in 0–60 cm), but with lower uncertainty (Dharumarajan et al., 2021). In fact, the coarser resolution of the

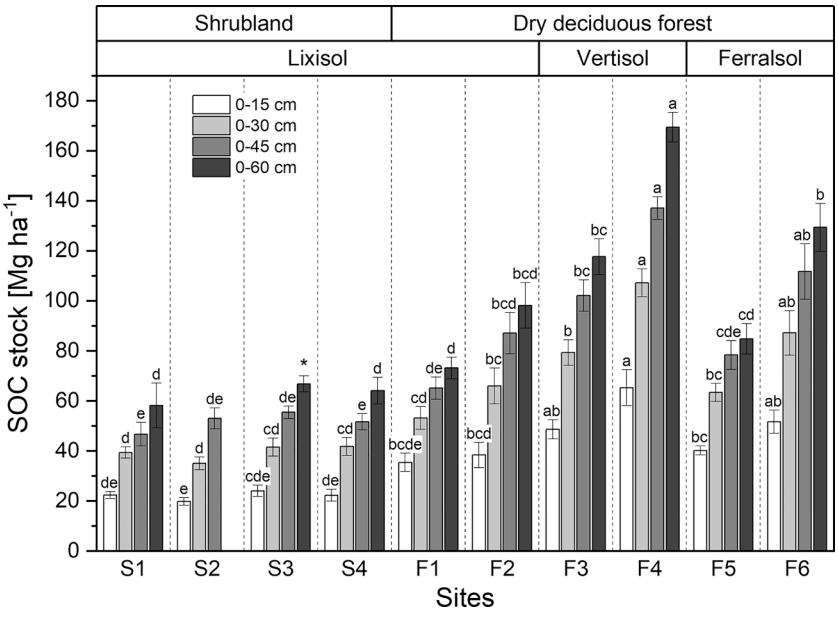

Fig. 2. Soil organic carbon (SOC) stocks [Mg ha^{-1}] up to 60 cm soil depth for each site. Sites S1-S2 represent Lixisols under shrubland, sites S3-S4 Lixisols under open-mixed shrubland/forest, sites F1-F2 Lixisols under tropical dry deciduous forest, sites F3-F4 Vertisols under tropical dry deciduous forest (site F3 Vertisol on gneiss and site F4 Vertisol on amphibolite) and sites F5-F6 Ferralsols (site F5 shallow Ferralsol) under tropical dry deciduous forest. Values represent the mean and error bars the variability (SE) ($n > 3$, except if marked with an asterisk $n = 2$). Letters indicate significant differences at $p < 0.05$. For SOC stock calculation, see Material and Method section.

cited study missed the SOC stock heterogeneity (ranging here from 73.2 to 169.4 Mg ha^{-1}) due to local variations in vegetation, geology and soil properties. This was depicted in the present study by high replication in small, contrasting watersheds; however, these small-scale watersheds cannot be considered as representative for the whole Western Ghats ecoregion as compared to Dharumarajan et al. (2021). If we would extrapolate our SOC stocks for sites (F4 and F6 respectively) where we have measured SOC contents up to 1 m (by approximating the BD for 60–100 cm from the average BD of 45–60 cm), the total SOC stock would account for 174.2 and 159.8 Mg ha^{-1} respectively (data not shown), which would fall in the range of SOC stocks up to 1 m depth predicted for deciduous forests (125–240 Mg ha^{-1}) across India (Nayak et al., 2020). Recent global estimates of SOC stocks in the first metre for tropical dry forests (130.7 ± 40.5 Mg ha^{-1}) were also comparable to our findings (Duarte-Guardia et al., 2019). Finally, the observed forest SOC stocks in this study were higher compared to early, field-based estimations of SOC stocks for tropical dry deciduous forest, which were ranging from 37.5 (0–50 cm) to 69.9 Mg ha^{-1} (0–100 cm) for India (Chhabra et al., 2003) or around 87.3 Mg ha^{-1} (0–60 cm) for the Eastern Ghats (Venkanna et al., 2014).

The SOC in subsoils (>30 cm) contributed to 35 % of the profile SOC stock (0–60 cm) under open-mixed shrubland/forest (S1-S4), and between 25 % (F5) and up to 37 % (F4) in the deciduous forest. This is in line with global estimates for the contribution of the SOC stock in subsoils (>20 cm) for the 0–60 cm interval for shrublands (41 %) and forests (34 %), and specifically for tropical deciduous forests (41 %; Jobbágy and Jackson (2000)). The contribution of subsoils down to 1 m (F3 and F6) accounted for 55 % and 46 % respectively (data not shown), which are lower compared to the 67 % of SOC in 20–100 cm suggested in Jobbágy and Jackson (2000). The soils studied here cumulated substantial amount of SOC below 30 cm despite their low SOC contents in subsoil layers (see section 3.2). Mechanisms explaining these subsoil SOC stocks are pedoturbation in case of Vertisols due to cracks (Fig. S1) induced by shrink-swelling given high clay contents of > 30 % and presence of smectite clays (Kurtzman et al., 2016; Zech et al., 2014). Bioturbation through termites can further cause translocation of organic matter in depth, which was frequently observed in the Lixisols and Ferralsols under shrubland and forest, but also the Vertisol (Fig. S2; see also Jouquet et al., 2016a; 2016b).

3.2. Soil organic carbon quality under different vegetation and land-use transitions

The SOC contents were generally higher in forest soils compared to soils under other vegetation, and decreased with soil depth for all sites (Fig. 3). The SOC contents in topsoils (0–15 cm) reached around 1.0 % for the Lixisol under shrubland (S1-S2). It ranged between 1.5 and 2.0 % for Lixisols under open-mixed shrubland/forest (S3-S4), and Lixisols (F1-F2) and the shallow Ferralsol (F5) under forest. They were > 2 % for the Vertisols (F3: 2.4 % and F4: 3.4 %) and the Ferralsol on gneiss (F6: 2.4 %) under forest in the top 15 cm. SOC contents always gradually decreased with increasing depth (>15 cm; Fig. 3) and ranged between 0.5 and 1.0 % below 45 cm for all sites, except the Vertisol on amphibolite (F4: 1.7 %) and the Ferralsol on gneiss (F6: 1.1 %). This decrease was more pronounced in the forest sites (F1-F6; Fig. 3), which could be attributed to differences in litter input and root depth distribution (Rumpel and Kögel-Knabner, 2011). Previous work in the research area showed SOC contents in the same range according to our findings (Violette et al., 2010a), but generally higher compared to a soil survey in the Eastern Ghats in south India for grasslands, shrublands and forests (0.1–1.7% SOC in 0–20 cm and 0.02–1.1 % SOC in 20–50 cm) (Fiener et al., 2014).

In the shrubland sites (S1-S2), the δ^{13}C of TOC became increasingly more negative with increasing soil depth (Fig. 3 and Table 2). This could be explained by fresh organic matter input in depth due to deep rooting of shrubs, bioturbation of frequently observed termites or management practices (Jouquet et al., 2016a; Rumpel and Kögel-Knabner, 2011; Violette et al., 2010b). In addition, we observed an increase in the cellulose/lignin ratio (e.g. from 1.1 (0–15 cm) to 6.4 (45–60 cm) in S1) along a decrease in the two aliphatic/aromatic ratios (e.g. from 1.5 (0–15 cm) to 1.1 (45–60 cm) in S1 for the aromatic peak at 880 cm^{-1}) with depth (Fig. 4). These trends could be related to an increase in aromaticity of SOC with depth through microbial decomposition (Rumpel and Kögel-Knabner, 2011), which would be in line with the slight decrease in C:N (from 11 to 12 (0–30 cm) to 10 (30–60 cm) in S1; Table 2) and the increase in δ^{13}C with depth (Fig. 3).

The Lixisols under open-mixed shrubland/forest (S3-S4) showed comparable δ^{13}C values to the shrubland sites (S1-S2) in the top 15 cm (Fig. 3). The values increased substantially in 15–45 cm, approaching the highest values (22 to −18 ‰), and subsequently decreased again slightly in 45–60 cm. The increase in 15–45 cm depth could be explained by substantial inputs of the most abundant C_4-grass species (*Heteropogon*

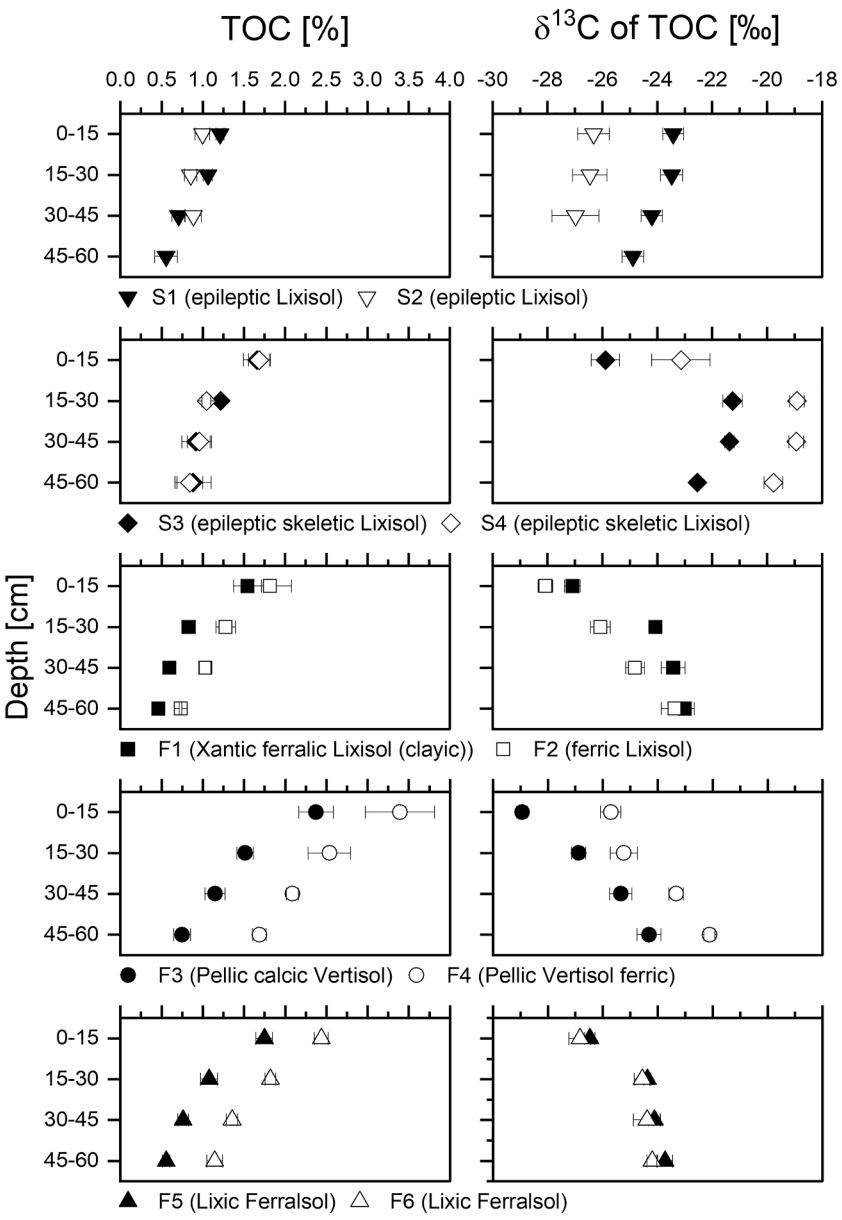

Fig. 3. Total organic carbon (TOC) content [%] and carbon isotopic ratio $^{13}C/^{12}C$ [‰] up to 60 cm depth for each site. Sites S1-S2 represent Lixisols under shrubland, sites S3-S4 Lixisols under open-mixed shrubland/forest, sites F1-F2 Lixisols under tropical dry deciduous forest, sites F3-F4 Vertisols under tropical dry deciduous forest (site F3 Vertisol on gneiss and site F4 Vertisol on amphibolite) and sites F5-F6 Ferralsols (site F5 shallow Ferralsol) under tropical dry deciduous forest. Values represent the mean and with standard error of the mean (SE) (n = 3–9, see Table 2).

contortus: measured $\delta^{13}C$ signal of −13.0 ± 0.2 ‰), which was in line with the sharp increase in cellulose/lignin ratios below 15 cm (from 1.3 (0–15 cm) to around 6 (15–60 cm) for site S4; Fig. 4). The decrease in $\delta^{13}C$ in 45–60 cm could be, similar to the shrubland sites (S1-S2; see above explanation), related to increasing proportions of root inputs of shrubs and/or more aromatic, microbial-processed SOC with depth in the open-mixed shrubland/forest sites, which was in line with the decrease in both aliphatic/aromatic ratios with depth (Fig. 4) and the decrease in C:N ratios with increasing depth (from 16.3 and 22.8 (0–15 cm) to 12.5 and 10.0 (45–60 cm) for sites S3-S4 respectively; Table 2). These findings direct to a potential grassland-dominated vegetation such as a tropical savannah in the past, which resulted in the increased $\delta^{13}C$ ratios below 15 cm. Or it represents a forest-savannah transition with a discontinuous tree canopy and continuous C_4-grass understory at present (Ratnam et al., 2011), where fresh organic matter with different origins enters (Boutton et al., 1998; Ladd et al., 2014), which resulted in a more negative $\delta^{13}C$ ratio in topsoils (Fig. 3).

The forest sites showed $\delta^{13}C$ ratios in topsoils of the mixed forest ecosystem (between −29 to −26 ‰ in 0–15 cm; F1-F6). This is in line with phytolith morphotypes composition (indicators for grass and forest biomass) extracted from topsoils in Mule Hole (Riotte et al., 2018). Below that, the $\delta^{13}C$ increased with increasing depth, approaching values between −24 to –22 ‰ (Fig. 3). Similar $\delta^{13}C$ depth trends were observed in soil cores of nearby tropical highlands (Nilgiri hills); while the SOC in topsoils showed a mixed C_3– and C_4-signal (from forest and grassland), the signal of C_4-vegetation (mainly grass) started dominating with depth (Caner et al., 2007; see also section 3.3.1). Further, we observed a slight increase of cellulose/lignin with depth (especially for the Vertisols (from 0.3 (0–15 cm) to 1.8 (45–60 cm) for F3); Fig. 4), which could be attributed to the relative enrichment of cellulose-rich organic matter (Rumpel and Kögel-Knabner, 2011). The C:N ratios, which showed a general increase with depth (Table 2) and highest values below 30 cm (F3: 14.2 (30–45 cm) and F4: 14.7 (45–60 cm)), indicated contribution of plant-derived compounds in the subsoil. These could originate from root inputs of shrubs or vertical transport of soluble, aromatic plant compounds through the profile (Rasse et al., 2005; Rumpel and Kögel-Knabner, 2011). In case of the Vertisols (F3-F4), pedoturbation and formation of cracks due to the shrink-swelling of smectite clays during dry season can be a main factor controlling the depth trends in $\delta^{13}C$ and C:N ratios (Zech et al., 2014), but also the

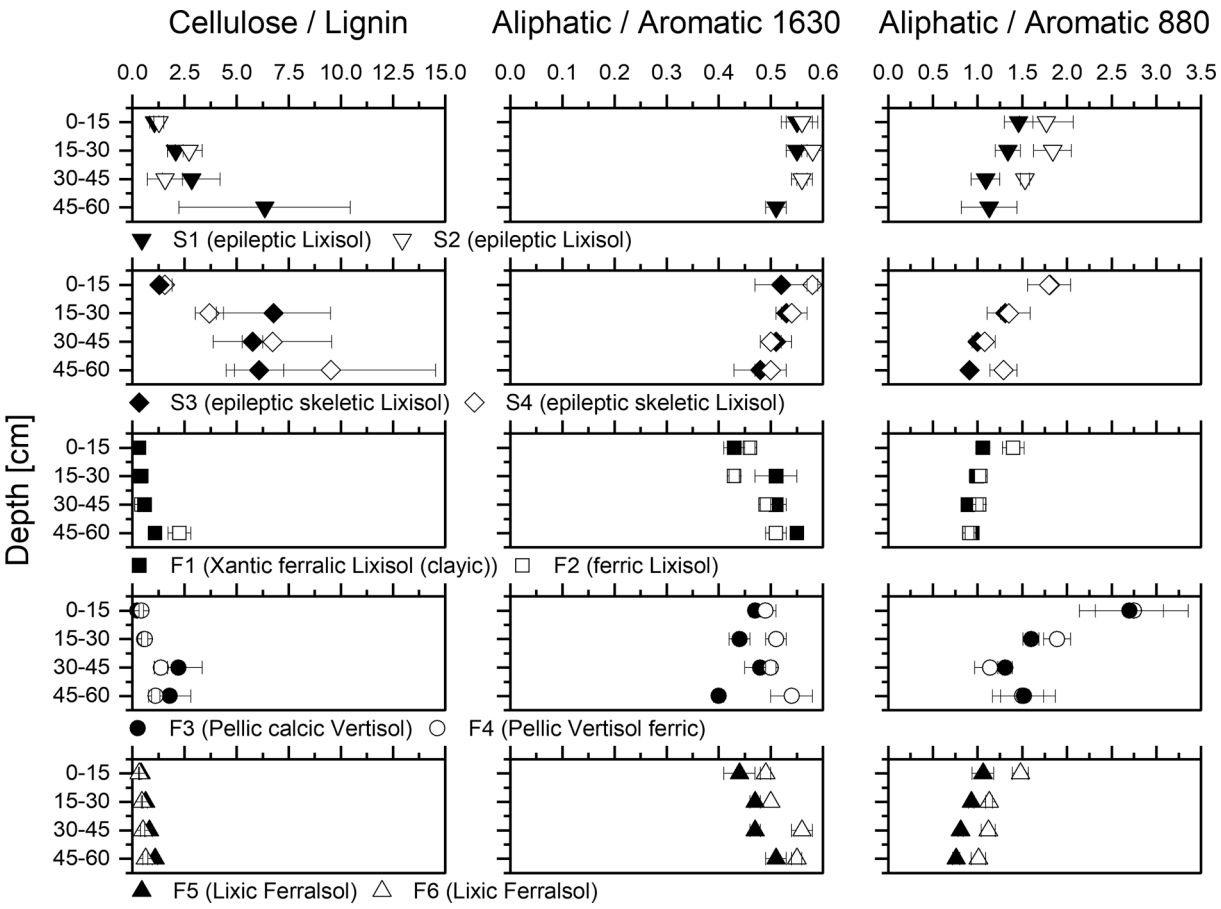

Fig. 4. Compound-specific ratios derived from diffuse reflectance infrared Fourier-transformed spectroscopy (DRIFT) analysis for the ten sites up to 60 cm depth. Selected maximum absorbance were in the range of 1260–1210 cm^{-1} for cellulose, 1510–1500 cm^{-1} for lignin, 2930–2850 cm^{-1} for aliphatic C–H, 1660–1600 cm^{-1} and 893–852 cm^{-1} for aromatic C = C (for details, see Material and Methods). Sites S1-S2 represent Lixisols under shrubland, sites S3-S4 Lixisols under open-mixed shrubland/forest, sites F1-F2 Lixisols under tropical dry deciduous forest, sites F3-F4 Vertisols under tropical dry deciduous forest (site F3 Vertisol on gneiss and site F4 Vertisol on amphibolite) and sites F5-F6 Ferralsols (site F5 shallow Ferralsol) under tropical dry deciduous forest. Values are means and error bars represent standard errors (n = 3–9, see Table 2).

relative proportion of subsoil SOC to the total SOC stock if organic matter falls down these cracks (Fig. S1 and section 3.1).

The litter composition of the most abundant forest species composition (ATT facies, see Table 1) on the common Ferralsol is mainly leave-derived (2840 kg litter mass ha^{-1}), followed by grass inputs (1540 kg litter mass ha^{-1}) and only to a smaller extent woody biomass (820 kg litter mass ha^{-1}) (Riotte et al., 2014). The large proportion of leave and grass inputs would explain the increase of the aliphatic/aromatic ratio using the aromatic peak at 1630 cm^{-1} (vegetation signal). The decrease of the aliphatic/aromatic ratio using the aromatic peak at 880 cm^{-1} in contrast could be attributed to the accumulation of aromatic compounds with depth (Fig. 4), and thus advanced degree of microbial decomposition in deeper soil horizons (Rumpel and Kögel-Knabner, 2011). A widespread invasion of the C_3-shrub lantana (*Lantana camara* (L.)) over the last decades has been observed in Mule Hole forest. This invasion could affect the SOC dynamics if it changes the composition of organic matter entering the soil from forest-dominated to shrub-dominated ecosystems with associated native biodiversity loss and the SOC stocks and depth distribution due to deep rooting profiles of shrubs (Mungi et al., 2020; Prasad, 2012; Ramaswami et al., 2013).

To conclude, our data on SOC quality (^{13}C, mid-infrared spectra and C:N ratios) indicated either alternating past vegetation before the dry deciduous forest in Mule Hole was established (see section 3.3.1 and Caner et al. (2007) and Sukumar et al. (1993)) or that the present forest lies at the edge of a forest-savannah transition common for tropical regions like in southwestern India, which has been discussed in ecological literature (Oliveras and Malhi, 2016; Ratnam et al., 2011).

3.3. Ecosystem properties driving soil organic carbon quantity and quality

3.3.1. Paleoclimate and soil organic carbon

High SOC stocks in Mule Hole forest (F1-F6) could have partially resulted from a tropical grassland/savannah in the past (Oliveras and Malhi, 2016; Ratnam et al., 2011). This could be supported with our findings on $\delta^{13}C$ depth profiles and mid-infrared data (see Figs. 3-4 and section 3.2) and/or evergreen and moist deciduous forests based on pollen data (Riotte et al., 2018). The undated pollen data in Riotte et al (2018) and the dated pedogenic carbonates from Violette et al. (2010b) indicate alternating pluri-millennial wet and (semi-) arid climatic conditions since the Last Glacial Maximum (±18′000 years BP) that would have allowed the vegetation to adapt, which could explain the quality of SOC over depth (i.e. the increase in $\delta^{13}C$ with depth in the forest sites).

Core samples from nearby tropical peats (Nilgiri hills) suggest more arid conditions dominated by C_4-vegetation (grassland/savannah) around the Last Glacial Maximum, more humid conditions dominated by C_3-vegetation (mainly forest) around 16′000-10′000 years BP and again a more arid phase between 10′000-6′000 years BP. Around 600–700 years BP, wet conditions occurred that allowed a moist forest cover in the region (Caner et al., 2007; Sukumar et al., 1993). In recent centuries, Mule Hole forest represented teak plantations (see Chitra-Tarak et al. (2015)), which were finally succeeded by a secondary forest originating from times before the country's independence (1947) and creation of the

National park (1973–74) 50–70 years ago. SOC stocks decreased with increasing forest succession in a tropical secondary forest in Cameroon with similar climate, and the contribution of understory C_4-grass to the total SOC stock (0–100 cm) also decreased, partially causing the lower SOC stocks in the old regrowth forest (Sugihara et al., 2019). In contrast, a change from a grassland-dominated ecosystem (pasture, savannah) to a secondary (regrowth) forest can lead to SOC stock increases by up to 17.5 % (+12.4 Mg ha^{-1}) (Don et al., 2011; Powers et al., 2011); however such increases are not systematic (Marin-Spiotta et al., 2009; Neumann-Cosel et al., 2011) and the transition between tropical savannah and secondary forest (and vice versa) is not linear, but a dynamic process depending on natural and anthropogenic factors (Oliveras and Malhi, 2016).

3.3.2. Geology and soil organic carbon

The largest SOC stock was found in the Vertisol on amphibolite (F4) and it was significantly higher compared to all other soils except for the first 45 cm of the Ferralsol on gneiss (F6) and the first 15 cm of the Vertisol on gneiss (F3; $p < 0.05$; Fig. 2). These differences in SOC stocks are possibly caused by differences in texture, mineral surface reactivity and impervious and anoxic layers of soils developed from mafic to ultramafic rocks such as the amphibolite (F4) compared to soils developed from the paragneiss (F1-F3 & F5-F6). The amphibolite, rich in Fe^{2+}, Mg^{2+} and Ca^{2+}, favours the formation of smectites and Fe-(oxyhydr) oxides as secondary clays in the Vertisol (F4; Table 2 and supplementary material), with concentrations of Ca- and Mg-smectites between 10 and 35 % depending on soil depth (Violette et al., 2010a). Thus, despite general rapid turnover of SOC in tropical soils, substantial amounts of SOC are stabilized by interaction with the high contents of smectites that show high surface area, high permanent negative surface charges and CEC, and that trap SOC in greater depth due to the formation of cracks through shrinking-swelling in the dry season (pedoturbation; see Fig. S1) in the Vertisol on amphibolite, but also in the Vertisol on gneiss (Bruun et al., 2010; Kurtzman et al., 2016; Nguetnkam et al., 2007).

3.3.3. Soil properties and soil organic carbon

We observed clear trends between the three studied major soil types; however, there were still substantial differences in SOC stocks between the two Vertisols (F3 and F4) or the two Ferralsols (F5 and F6) despite being attributed to the same soil class (Fig. 2). This stresses out the importance of pedon-specific SOC dynamics and soil forming parent material.

When considering all soil depths (0–60 cm), we found a weak and not significant correlation of clay content with SOC stock (Pearson's $r = 0.21$) and SOC contents (Pearson's $r = 0.28$; Fig. S3 and supplementary material). If assessed for individual depths, clay content was strongly correlated with SOC stock, SOC content and TN content for the first three depths up to 45 cm (Pearson's r: 0.7–0.9 and $p < 0.05$; data not shown); however our sample size, especially for individual soil layers, limits the interpretation of these results because of the analysis of composite samples for soil properties. Recent studies suggest that clay mineralogy could be more important than clay content because of its control on active, specific surface area (Bruun et al., 2010; Vaughan et al., 2019) and thus could explain the SOC stock differences between the two Vertisols (F3 and F4), but also between the soil types under forest (F1-F6). As an example, the Vertisol on amphibolite (F4) showed higher Fe_2O_3 and MgO contents than the Vertisol on gneiss (F3; see Table 2 and supplementary material) and is consequently dominated by smectite clays, whereas the Vertisol on gneiss is dominated by the continuum from kaolinite to interstratified kaolinite-smectite clays (Pulla et al., 2016; Riotte et al., 2014). Vertisols show volumetric contents of smectite up to 35 % or even > 50 % and between 13 and 28 % of kaolinite, whereas the Ferralsols and Lixisols show kaolinite contents of 38–64 % (Violette et al., 2010a; Zech et al., 2014). However, it has been shown that smectite-dominated tropical soils are not stabilizing more SOC compared to kaolinite-dominated soils (Bruun et al., 2010), which can be confirmed by our results where the SOC stocks of the Vertisol on gneiss (F4) is not significantly different from the stocks of the Ferralsols on gneiss (F5-F6) for the same geology (Fig. 2; $p > 0.05$).

The two Vertisols (F3-F4) and the Ferralsol (F6) with the highest SOC stocks showed highest silt and lowest sand contents respectively (Fig. 2 and Table 2). Silt showed a strong positive (Pearson's r: 0.6–0.7 and $p < 0.05$) and sand a moderate negative (Pearson's r: − 0.4–0.5 and $p < 0.05$) correlations with SOC stocks, SOC contents and TN contents in the full dataset (Fig. S3 and supplementary material), but also in individual soil layers. For silt, the positive correlation was even stronger for the first layer (0–15 cm: Pearson's $r \pm 0.9$ and $p < 0.05$; data not shown). Positive correlations of silt with SOC have been previously found in tropical soils (van Noordwijk et al., 1997; Vaughan et al., 2019). In case of sand, the negative correlation became even stronger for the first three horizons (Pearson's r: − 0.75–0.95 and $p < 0.05$; see Fig. S3), possibly due to limited mineral surface reactivity of coarser particles (Barthès et al., 2008).

The Vertisol on amphibolite (F4) with the highest SOC stock (Fig. 2) showed the highest total Fe_2O_3 contents after the Ferralsol on gneiss (F6; Table 2); however, association of Fe_2O_3 contents with SOC stocks (Pearson's r: 0.1) and TN contents (Pearson's r: 0.1) were negligible and weak with SOC contents (Pearson's r: 0.3; Fig. S3). It has to be noted that we estimated total oxide contents with XRF data and not extractable Fe-(oxyhdr)oxides. Comparable SOC stocks between the Ferralsol (F6) and Vertisol (F3) on gneiss, the latter showing higher contents of clay and higher CEC, could be related to the interactions between Fe-(oxyhdr) oxides and kaolinite clays. In soils derived from sedimentary rocks (such as the Precambrian peninsular gneiss), containing mainly goethite and hematite (Wiriyakitnateekul et al., 2007), Fe-(oxyhdr)oxides can increase the SOC stabilization of kaolinite through increases in specific surface area of kaolinite with lower surface reactivity (Bruun et al., 2010; Kirsten et al., 2021). Total Al_2O_3 contents were moderately, negatively correlated with SOC stocks, SOC content and TN content in the full dataset and for the first 0–15 cm (Pearson's r: − 0.4–0.6 and $p < 0.05$) and were lower in the Vertisols compared to other soil types (Fig. S3 and Table 2). In addition, Vertisols also showed the lowest SiO_2 contents (Table 2), especially the Vertisol on amphibolite (F4), which is linked to the formation of smectite clays through weathering of feldspars and biotite and thus depletion of Si (Nguetnkam et al., 2007; Riotte et al., 2018).

SOC stocks and TN contents showed weak, negative (Pearson's r: − 0.2–0.3 and $p > 0.05$) and SOC contents moderate, negative (Pearson's r: − 0.42 and $p < 0.05$) associations with SiO_2 (Fig. S3 and supplementary material). Furthermore, K_2O and Na_2O contents showed negative correlations in the full dataset and individual soil layers that were moderate for SOC stocks and contents (Pearson's r: − 0.2–0.4), and negligible for TN contents (Pearson's r: < 0.2), but mostly not significant (Fig. S3 and supplementary material). The negative correlation of these elements with SOC is related to the fact that we analysed total elemental contents of K_2O and Na_2O, which are present mostly in primary minerals like Na-plagioclase or sericite that are highly resistant to weathering, and not its contribution to the CEC (Riotte et al., 2018).

The effective CEC displayed moderate positive associations with SOC stock, SOC contents and TN contents in the whole dataset (Pearson's r: < 0.6 and $p < 0.05$; Fig. S3), and this was more pronounced in the first two layers (data not shown). The CEC was highest in the Vertisols (F3-F4; Table 2), especially in the Vertisol on gneiss (F3), but the measured CEC values were low and of relative low range compared to the literature (e.g. Zech et al. (2014)). The high CEC in the Vertisol on gneiss (F3) can be attributed to the presence of substantial amounts of Ca^{2+} (up to 5 % CaO; see supplementary material) through secondary carbonates (calcite) (Violette et al., 2010b), which can be an important SOC stabilisation factor (Rowley et al., 2018). The high CEC of the Vertisol on amphibolite can be related to the smectite assemblage (Bruun et al., 2010), which also showed the highest SOC stock (Fig. 2). The pH did not vary substantially between soil types and depths (between 5 and 6),

except the deeper layers of the Vertisol on gneiss that contained secondary carbonates and some of the Lixisols under shrubland (pH > 6; see Table 2 and supplementary material).

3.3.4. Landform position and soil organic carbon

The SOC stocks under forest gradually increased from upslope positions (F1) over intermediate plots (F2) towards the valley, and the SOC stocks in soils close to the stream (F3) were significantly different from the uppermost plot on the hillslope (Fig. 2; $p < 0.05$). High SOC stocks in the Vertisol on gneiss (F3) can thus be explained by the landform position as it lies in a depositional area with possibly reduced decomposition rates and higher C inputs from litter or eroded material from upslope (Berhe et al., 2018). This is not the case for the Vertisol on amphibolite (F4), which is located on elevated position on the crest line.

4. Conclusion

SOC dynamics in tropical plant-soil systems are poorly understood, yet extremely important in the global C cycle and sensitive to perturbations such as climate and land-use change. The SOC stocks in three small-scale sub-humid and semi-arid watersheds in southwestern India showed a large range from 58.2 to 169.4 Mg ha^{-1} in the first 60 cm, with differences depending on vegetation type and history, geology and soil properties. Contrary to general perception, tropical soils in this study store a substantial amount of SOC below 30 cm (up to 40 %), which needs to be taken into account in existing SOC inventories. Ferralsols, which are generally perceived to be low in SOC, showed substantial SOC stocks, in some cases even in the same range than some of the Vertisols under the same forest cover and geology. This puts forward the fact that no general conclusions can be inferred from (sub-) regional proxies such as climate or larger soil groups, but that at the field/landscape scale considered in the present study, it seems apparent that the interaction of geology, soil physico-chemical properties, vegetation dynamics and landform are overriding the importance of climate for tropical SOC dynamics.

A combination of carbon (TOC, ^{13}C), C:N, mid-infrared assessments allowed to identify the historical vegetation dynamics and land-use transitions in the studied watersheds, which were in line with other proxies reported in the literature. The vegetation history points at least in Mule Hole forest towards a shift from former moist, evergreen forest succeeded by a tropical savannah, to secondary (regrowth) dry deciduous forest, but the historical sequence cannot be determined in conclusion. If the interpreted vegetation signals are not past ones, this could infer that the studied Mule Hole watershed lies at the transition between tropical savannah and secondary dry deciduous forest with contributions of C_4-grass understory to the overall C signal of the forest. Our study provides additional data on SOC quantity and quality from small-scale tropical watersheds and forms the basis for more in-depth studies looking at the controlling factors of SOC quality in tropical (forested) ecosystems.

Declaration of Competing Interest

The authors declare that they have no known competing financial interests or personal relationships that could have appeared to influence the work reported in this paper.

Acknowledgements

Monitoring and maintenance of the watersheds in the Kabini Critical Zone Observatory Multiscale Tropical Catchments (M-TROPICS), founded by several French institutions (i.e. IRD, CNRS, UPS), is hosted at the Indo-French Cell for Water Sciences and the Department of Civil Engineering at the Indian Institute of Science in Bangalore in close collaboration with the Karnataka Forest Department and Bandipur National Park staff. The authors acknowledge the field assistance of Benjamin Baud and Dr. Cécile Gomez, the staff of the Indo-French Cell for Water Sciences for material acquisition and laboratory assistance, and the field assistance and protection of local people of Maddur colony during fieldwork. In addition, support of the Karnataka Forest Department, Bandipur National Park and ICAR-National Bureau of Soil Survey and Land Use Planning Regional Centre staff is highly appreciated.

Funding

This work was supported by the Swiss National Science Foundation [grant no. 200021_178768].

Data availability

The data related to this article are available upon request from the corresponding author and available online on Zenodo (10.5281/zenodo.5675793).

Appendix A. Supplementary data

Supplementary data to this article can be found online at https://doi.org/10.1016/j.geoderma.2021.115606.

References

Barbiéro, L., Parate, H.R., Descloitres, M., Bost, A., Furian, S., Mohan Kumar, M.S., Kumar, C., Braun, J.-J., 2007. Using a structural approach to identify relationships between soil and erosion in a semi-humid forested area, South India. Catena 70 (3), 313–329. https://doi.org/10.1016/j.catena.2006.10.013.

Barthès, B.G., Kouakoua, E., Larré-Larrouy, M.-C., Razafimbelo, T.M., de Luca, E.F., Azontonde, A., Neves, C.S.V.J., de Freitas, P.L., Feller, C.L., 2008. Texture and sesquioxide effects on water-stable aggregates and organic matter in some tropical soils. Geoderma 143 (1-2), 14–25. https://doi.org/10.1016/j.geoderma.2007.10.003.

Batjes, N.H., 2016. Harmonized soil property values for broad-scale modelling (WISE30sec) with estimates of global soil carbon stocks. Geoderma 269, 61–68. https://doi.org/10.1016/j.geoderma.2016.01.034.

Batjes, N.H., Ribeiro, E., van Oostrum, A., 2020. Standardised soil profile data to support global mapping and modelling (WoSIS snapshot 2019). Earth Syst. Sci. Data 12, 299–320. https://doi.org/10.5194/essd-12-299-2020.

Beer, C., Reichstein, M., Tomelleri, E., Ciais, P., Jung, M., Carvalhais, N., Rödenbeck, C., Arain, M.A., Baldocchi, D., Bonan, G.B., Bondeau, A., Cescatti, A., Lasslop, G., Lindroth, A., Lomas, M., Luyssaert, S., Margolis, H., Oleson, K.W., Roupsard, O., Veenendaal, E., Viovy, N., Williams, C., Woodward, F.I., Papale, D., 2010. Terrestrial gross carbon dioxide uptake: global distribution and covariation with climate. Science 329 (5993), 834–838. https://doi.org/10.1126/science:1184984.

Berhe, A.A., Barnes, R.T., Six, J., Marín-Spiotta, E., 2018. Role of soil erosion in biogeochemical cycling of essential elements: carbon, nitrogen, and phosphorus. Annu. Rev. Earth Planet. Sci. 46 (1), 521–548. https://doi.org/10.1146/earth.2018.46.issue-110.1146/annurev-earth-082517-010018.

Bhattacharyya, T., Ray, S.K., Pal, D.K., Chandran, P., Mandal, C., Wani, S.P., 2009. Soil carbon stocks in India — issues and priorities. J. Indian Soc. Soil Sci. 57, 461–468. http://krishi.icar.gov.in/jspui/handle/123456789/36617.

Boutton, T.W., Archer, S.R., Midwood, A.J., Zitzer, S.F., Bol, R., 1998. d 13C values of soil organic carbon and their use in documenting vegetation change in a subtropical savanna ecosystem. Geoderma 82, 5–41. https://doi.org/10.1016/S0016-7061(97)00095-5.

Braun, J.-J., Descloitres, M., Riotte, J., Fleury, S., Barbiéro, L., Boeglin, J.-L., Violette, A., Lacarce, E., Ruiz, L., Sekhar, M., Mohan Kumar, M.S., Subramanian, S., Dupré, B., 2009. Regolith mass balance inferred from combined mineralogical, geochemical and geophysical studies: Mule Hole gneissic watershed, South India. Geochim. Cosmochim. Acta 73 (4), 935–961. https://doi.org/10.1016/j.gca.2008.11.013.

Bruun, T.B., Elberling, B.o., Christensen, B.T., 2010. Lability of soil organic carbon in tropical soils with different clay minerals. Soil Biol. Biochem. 42 (6), 888–895. https://doi.org/10.1016/j.soilbio.2010.01.009.

Caner, L., Seen, D.L., Gunnell, Y., Ramesh, B.R., Bourgeon, G., 2007. Spatial heterogeneity of land cover response to climatic change in the Nilgiri highlands (Southern India) since the last glacial maximum. The Holocene 17 (2), 195–205. https://doi.org/10.1177/0959683607075833.

Carter, M.R., Gregorich, E.G. (Eds.), 2008. Soil sampling and methods of analysis, 2nd ed. CRC Press, Talyor & Francis Group, Boca Raton, Florida USA. https://doi.org/10.1201/9781420005271.

Carvalhais, N., Forkel, M., Khomik, M., Bellarby, J., Jung, M., Migliavacca, M., Mu, M., Saatchi, S., Santoro, M., Thurner, M., Weber, U., Ahrens, B., Beer, C., Cescatti, A., Randerson, J.T., Reichstein, M., 2014. Global covariation of carbon turnover times with climate in terrestrial ecosystems. Nature 514 (7521), 213–217. https://doi.org/10.1038/nature13731.

Chatterjee, S., Santos, F., Abiven, S., Itin, B., Stark, R.E., Bird, J.A., 2012. Elucidating the chemical structure of pyrogenic organic matter by combining magnetic resonance, mid-infrared spectroscopy and mass spectrometry. Org Geochem. 51, 35–44. https://doi.org/10.1016/j.orggeochem.2012.07.006.

Chhabra, A., Palria, S., Dadhwal, V.K., 2003. Soil organic carbon pool in Indian forests. For. Ecol. Manage. 173 (1-3), 187–199. https://doi.org/10.1016/S0378-1127(02)00016-6.

Chitra-Tarak, R., Ruiz, L., Pulla, S., Dattaraja, H.S., Suresh, H.S., Sukumar, R., 2015. And yet it shrinks: A novel method for correcting bias in forest tree growth estimates caused by water-induced fluctuations. For. Ecol. Manage. 336, 129–136. https://doi.org/10.1016/j.foreco.2014.10.007.

Dharumarajan, S., Kalaiselvi, B., Suputhra, A., Lalitha, M., Vasundhara, R., Kumar, K.S.A., Nair, K.M., Hegde, R., Singh, S.K., Lagacherie, P., 2021. Digital soil mapping of soil organic carbon stocks in Western Ghats. South India. Geoderma Regional 25, e00387. https://doi.org/10.1016/j.geodrs.2021.e00387.

Don, A., Schumacher, J., Freibauer, A., 2011. Impact of tropical land-use change on soil organic carbon stocks - a meta-analysis. Glob. Change Biol. 17, 1658–1670. https://doi.org/10.1111/j.1365-2486.2010.02336.x.

Drake, T.W., Van Oost, K., Barthel, M., Bauters, M., Hoyt, A.M., Podgorski, D.C., Six, J., Boeckx, P., Trumbore, S.E., Cizungu Ntaboba, L., Spencer, R.G.M., 2019. Mobilization of aged and biolabile soil carbon by tropical deforestation. Nat. Geosci. 12 (7), 541–546. https://doi.org/10.1038/s41561-019-0384-9.

Duarte-Guardia, S., Peri, P.L., Amelung, W., Sheil, D., Laffan, S.W., Borchard, N., Bird, M.I., Dieleman, W., Pepper, D.A., Zutta, B., Jobbagy, E., Silva, L.C.R., Bonser, S.P., Berhongaray, G., Piñeiro, G., Martinez, M.-J., Cowie, A.L., Ladd, B., 2019. Better estimates of soil carbon from geographical data: a revised global approach. Mitig Adapt Strateg Glob Change 24 (3), 355–372. https://doi.org/10.1007/s11027-018-9815-y.

Dungait, J.A.J., Hopkins, D.W., Gregory, A.S., Whitmore, A.P., 2012. Soil organic matter turnover is governed by accessibility not recalcitrance. Glob. Change Biol. 18 (6), 1781–1796. https://doi.org/10.1111/gcb.2012.18.issue-610.1111/j.1365-2486.2012.02665.x.

Fiener, P., Gottfried, T., Sommer, M., Steger, K., 2014. Soil organic carbon patterns under different land uses in South India. Geoderma Regional 2–3, 91–101. https://doi.org/10.1016/j.geodrs.2014.10.005.

Flores, B.M., Staal, A., Jakovac, C.C., Hirota, M., Holmgren, M., Oliveira, R.S., 2020. Soil erosion as a resilience drain in disturbed tropical forests. Plant Soil 450 (1-2), 11–25. https://doi.org/10.1007/s11104-019-04097-8.

González-Domínguez, B., Niklaus, P.A., Studer, M.S., Hagedorn, F., Wacker, L., Haghipour, N., Zimmermann, S., Walthert, L., McIntyre, C., Abiven, S., 2019. Temperature and moisture are minor drivers of regional-scale soil organic carbon dynamics. Sci. Rep. 9, 1–11. https://doi.org/10.1038/s41598-019-42629-5.

Grace, J., Mitchard, E., Gloor, E., 2014. Perturbations in the carbon budget of the tropics. Glob. Change Biol. 20 (10), 3238–3255. https://doi.org/10.1111/gcb.2014.20.issue-1010.1111/gcb.12600.

Gunnell, Y., Bourgeon, G., 1997. Soils and climatic geomorphology on the Karnataka plateau, peninsular India. Catena 29 (3–4), 239–262. https://doi.org/10.1016/S0341-8162(96)00070-7.

Gupta, R.K., Rao, D.L.N., 1994. Potential of wastelands for sequestering carbon by reforestation. Curr. Sci. 66, 378–380. https://www.jstor.org/stable/24098762.

Hombegowda, H.C., van Straaten, O., Köhler, M., Hölscher, D., 2016. On the rebound: Soil organic carbon stocks can bounce back to near forest levels when agroforests replace agriculture in southern India. Soil 2 (1), 13–23. https://doi.org/10.5194/soil-2-13-2016.

Jobbágy, E.G., Jackson, R.B., 2000. The vertical distribution of soil organic carbon and its relation to climate and vegetation. Ecol. Appl. 10 (2), 423–436. https://doi.org/10.1890/1051-0761(2000)010[0423:TVDOSO]2.0.CO;2.

Jouquet, P., Bottinelli, N., Shanbhag, R.R., Bourguignon, T., Traoré, S., Abbasi, S.A., 2016a. Termites: The Neglected Soil Engineers of Tropical Soils. Soil Sci. 181, 157–165. https://doi.org/10.1097/SS.0000000000000119.

Jouquet, P., Chintakunta, S., Bottinelli, N., Subramanian, S., Caner, L., 2016b. The influence of fungus-growing termites on soil macro and micro-aggregates stability varies with soil type. Appl. Soil Ecol. 101, 117–123. https://doi.org/10.1016/j.apsoil.2016.02.001.

Kirsten, M., Mikutta, R., Vogel, C., Thompson, A., Mueller, C.W., Kimaro, D.N., Bergsma, H.L.T., Feger, K.-H., Kalbitz, K., 2021. Iron oxides and aluminous clays selectively control soil carbon storage and stability in the humid tropics. Sci Rep 11, 5076. https://doi.org/10.1038/s41598-021-84777-7.

Köchy, M., Hiederer, R., Freibauer, A., 2015. Global distribution of soil organic carbon – Part 1: Masses and frequency distributions of SOC stocks for the tropics, permafrost regions, wetlands, and the world. Soil 1 (1), 351–365. https://doi.org/10.5194/soil-1-351-2015.

Kurtzman, D., Baram, S., Dahan, O., 2016. Soil–aquifer phenomena affecting groundwater under vertisols: a review. Hydrol. Earth Syst. Sci. 20, 1–12. https://doi.org/10.5194/hess-20-1-2016.

Ladd, B., Peri, P.L., Pepper, D.A., Silva, L.C.R., Sheil, D., Bonser, S.P., Laffan, S.W., Amelung, W., Ekblad, A., Eliasson, P., Bahamonde, H., Duarte-Guardia, S., Bird, M., Cornelissen, H., 2014. Carbon isotopic signatures of soil organic matter correlate with leaf area index across woody biomes. J Ecol 102 (6), 1606–1611. https://doi.org/10.1111/jec.2014.102.issue-610.1111/1365-2745.12309.

Laub, M., Demyan, M.S., Nkwain, Y.F., Blagodatsky, S., Kätterer, T., Piepho, H.-P., Cadisch, G., 2020. DRIFTS band areas as measured pool size proxy to reduce parameter uncertainty in soil organic matter models. Biogeosciences 17 (6), 1393–1413. https://doi.org/10.5194/bg-17-1393-2020.

Maréchal, J.-C., Varma, M.R.R., Riotte, J., Vouillamoz, J.-M., Kumar, M.S.M., Ruiz, L., Sekhar, M., Braun, J.-J., 2009. Indirect and direct recharges in a tropical forested watershed: Mule Hole, India. J. Hydrol. 364 (3-4), 272–284. https://doi.org/10.1016/j.jhydrol.2008.11.006.

Marin-Spiotta, E., Silver, W.L., Swanston, C.W., Ostertag, R., 2009. Soil organic matter dynamics during 80 years of reforestation of tropical pastures. Glob. Change Biol. 15, 1584–1597. https://doi.org/10.1111/j.1365-2486.2008.01805.x.

Mehta, V.K., Sullivan, P.J., Walter, M.T., Krishnaswamy, J., DeGloria, S.D., 2008. Impacts of disturbance on soil properties in a dry tropical forest in Southern India. Ecohydrol. 1 (2), 161–175. https://doi.org/10.1002/eco.v1:210.1002/eco.15.

Mishra, U., Riley, W.J., 2015. Scaling impacts on environmental controls and spatial heterogeneity of soil organic carbon stocks. Biogeosciences 12 (13), 3993–4004. https://doi.org/10.5194/bg-12-3993-2015.

Mungi, N.A., Qureshi, Q., Jhala, Y.V., 2020. Expanding niche and degrading forests: Key to the successful global invasion of Lantana camara (sensu lato). Global Ecol. Conserv. 23, e01080. https://doi.org/10.1016/j.gecco.2020.e01080.

Nayak, R.K., Bhuvanachandra, A., Krishnapriya, M., Swapna, M., Patel, N.R., Tommar, A., Seshasai, M.V.R., Dadhwal, V.K., 2020. Spatiotemporal Variability of Soil Organic Carbon Content Over India Based on an Ecosystem Model and Regional Databases. J Indian Soc Remote Sens 48 (4), 553–561. https://doi.org/10.1007/s12524-019-01096-1.

Neumann-Cosel, L., Zimmermann, B., Hall, J.S., van Breugel, M., Elsenbeer, H., 2011. Soil carbon dynamics under young tropical secondary forests on former pastures—A case study from Panama. For. Ecol. Manage. 261 (10), 1625–1633. https://doi.org/10.1016/j.foreco.2010.07.023.

Nguetnkam, J.P., Kamga, R., Villiéras, F., Ekodeck, G.E., Yvon, J., 2007. Pedogenic formation of smectites in a vertisol developed from granitic rock from Kaélé (Cameroon, Central Africa). Clay miner. 42 (4), 487–501. https://doi.org/10.1180/claymin.2007.042.4.07.

Oliveras, I., Malhi, Y., 2016. Many shades of green: the dynamic tropical forest–savannah transition zones. Phil. Trans. R. Soc. B 371 (1703), 20150308. https://doi.org/10.1098/rstb.2015.0308.

Poeplau, C., Vos, C., Don, A., 2017. Soil organic carbon stocks are systematically overestimated by misuse of the parameters bulk density and rock fragment content. Soil 3 (1), 61–66. https://doi.org/10.5194/soil-3-61-2017.

Poker, J., MacDicken, K., 2016. Tropical Forest Resources: Facts and Tables. In: Pancel, L., Köhl, M. (Eds.), Tropical Forestry Handbook. Springer, Berlin, Heidelberg, pp. 3–45. https://doi.org/10.1007/978-3-642-54601-3_7.

Powers, J.S., Corre, M.D., Twine, T.E., Veldkamp, E., 2011. Geographic bias of field observations of soil carbon stocks with tropical land-use changes precludes spatial extrapolation. Proc. Natl. Acad. Sci. 108 (15), 6318–6322. https://doi.org/10.1073/pnas.1016774108.

Prasad, A.E., 2012. Landscape-scale relationships between the exotic invasive shrub *Lantana camara* and native plants in a tropical deciduous forest in southern India. J. Trop. Ecol. 28 (1), 55–64. https://doi.org/10.1017/S0266467411000563.

Proulx, R., Rheault, G., Bonin, L., Roca, I.T., Martin, C.A., Desrochers, L., Seiferling, I., 2015. How much biomass do plant communities pack per unit volume? PeerJ 3 (e849), 1–10. https://doi.org/10.7717/peerj.849.

Pulla, S., Riotte, J., Suresh, H.S., Dattaraja, H.S., Sukumar, R., Hui, D., 2016. Controls of soil spatial variability in a dry tropical forest. PLoS ONE 11 (4), e0153212. https://doi.org/10.1371/journal.pone.0153212.

R Core Team, 2020. R: A Language and Environment for Statistical Computing. R Foundation for Statistical Computing, Vienna, Austria. https://www.R-project.org/.

Ramaswami, G., Sukumar, R., Hewitt, J., 2013. Long-Term Environmental Correlates of Invasion by Lantana camara (Verbenaceae) in a Seasonally Dry Tropical Forest. PLoS ONE 8 (10), e76995. https://doi.org/10.1371/journal.pone.0076995.

Ramirez, P.B., Calderón, F.J., Haddix, M., Lugato, E., Cotrufo, M.F., 2021. Using Diffuse Reflectance Spectroscopy as a High Throughput Method for Quantifying Soil C and N and Their Distribution in Particulate and Mineral-Associated Organic Matter Fractions. Front. Environ. Sci. 9 (634472), 1–13. https://doi.org/10.3389/fenvs.2021.634472.

Rasse, D.P., Rumpel, C., Dignac, M.-F., 2005. Is soil carbon mostly root carbon? Mechanisms for a specific stabilisation. Plant Soil 269 (1-2), 341–356. https://doi.org/10.1007/s11104-004-0907-y.

Ratnam, J., Bond, W.J., Fensham, R.J., Hoffmann, W.A., Archibald, S., Lehmann, C.E.R., Anderson, M.T., Higgins, S.I., Sankaran, M., 2011. When is a 'forest' a savanna, and why does it matter?: When is a 'forest' a savanna. Glob. Ecol. Biogeogr. 20, 653–660. https://doi.org/10.1111/j.1466-8238.2010.00634.x.

Riotte, J., Maréchal, J.C., Audry, S., Kumar, C., Bedimo Bedimo, J.P., Ruiz, L., Sekhar, M., Cisel, M., Chitra Tarak, R., Varma, M.R.R., Lagane, C., Reddy, P., Braun, J.J., 2014. Vegetation impact on stream chemical fluxes: Mule Hole watershed (South India). Geochim. Cosmochim. Acta 145, 116–138. https://doi.org/10.1016/j.gca.2014.09.015.

Riotte, J., Meunier, J.D., Zambardi, T., Audry, S., Barboni, D., Anupama, K., Prasad, S., Chmeleff, J., Poitrasson, F., Sekhar, M., Braun, J.J., 2018. Processes controlling silicon isotopic fractionation in a forested tropical watershed: Mule Hole Critical Zone Observatory (Southern India). Geochim. Cosmochim. Acta 228, 301–319. https://doi.org/10.1016/j.gca.2018.02.046.

Riotte, J., Ruiz, L., Audry, S., Baud, B., Bedimo Bedimo, J., Boithias, L., Braun, J., Dupré, B., Duprey, J., Faucheux, M., Lagane, C., Marechal, J., Moger, H., Mohan Kumar, M.S., Parate, H., Ribolzi, O., Rochelle-Newall, E., Sriramulu, B., Varma, M., Sekhar, M., 2021. The Multiscale TROPIcal CatchmentS critical zone observatory M-TROPICS dataset III: Hydyro-geochemical monitoring of the Mule Hole catchment, south India. Hydrol. Process. 35 (e14196), 1–8. https://doi.org/10.1002/hyp.14196.

Robert, M., Thomas, A., Sekhar, M., Badiger, S., Ruiz, L., Willaume, M., Leenhardt, D., Bergez, J.-E., 2017. Farm typology in the Berambadi Watershed (India): Farming systems are determined by farm size and access to groundwater. Water 9 (51), 1–21. https://doi.org/10.3390/w9010051.

Rowley, M.C., Grand, S., Verrecchia, É.P., 2018. Calcium-mediated stabilisation of soil organic carbon. Biogeochemistry 137 (1-2), 27–49. https://doi.org/10.1007/s10533-017-0410-1.

Rumpel, C., Kögel-Knabner, I., 2011. Deep soil organic matter—a key but poorly understood component of terrestrial C cycle. Plant Soil 338, 143–158. https://doi.org/10.1007/s11104-010-0391-5.

Sekhar, M., Riotte, J., Ruiz, L., Jouquet, P., Braun, J.J., 2016. Influences of climate and agriculture on water and biogeochemical cycles: Kabini critical zone observatory. Proceedings of the Indian National Science Academy 82, 833–846. https://doi.org/10.16943/ptinsa/2016/48488.

Sugihara, S., Shibata, M., Mvondo Ze, A.D., Tanaka, H., Kosaki, T., funakawa, S., 2019. Forest understories controlled the soil organic carbon stock during the fallow period in African tropical forest: a 13C analysis. Sci. Rep. 9, 1–9. https://doi.org/10.1038/s41598-019-46406-2.

Sukumar, R., Ramesht, R., Pantt, R.K., 1993. A d13C record of late Quaternary climate change from tropical peats in southern India. Nature 364, 703–706. https://doi.org/10.1038/364703a0.

Torn, M.S., Swanston, C.W., Castanha, C., Trumbore, S.E., 2009. Storage and Turnover of Organic Matter in Soil. In: Senesi, N., Xing, B., Huang, M. (Eds.), Biophysico-Chemical Processes Involving Natural Nonliving Organic Matter in Environmental Systems. John Wiley & Sons, Inc, Hoboken, New Jersey, pp. 219–272. https://doi.org/10.1002/9780470494950.ch6.

van Noordwijk, M., Cerri, C., Woomer, P.L., Nugroho, K., Bernoux, M., 1997. Soil carbon dynamics in the humid tropical forest zone. Geoderma 79, 187–225. https://doi.org/10.1016/S0016-7061(97)00042-6.

Vaughan, E., Matos, M., Ríos, S., Santiago, C., Marín-Spiotta, E., 2019. Clay and climate are poor predictors of regional-scale soil carbon storage in the US Caribbean. Geoderma 354, 113841. https://doi.org/10.1016/j.geoderma.2019.06.044.

Venkanna, K., Mandal, U.K., Solomon Raju, A.J., Sharma, K.L., Adake, R.V., Pushpanjali, Sanjeeva Reddy, B., Masane, R.N., Venkatravamma, K., Peda Babu, B., 2014. Carbon stocks in major soil types and land-use systems in semiarid tropical region of southern India. Current Science 106, 604–611. https://www.jstor.org/stable/24100069.

Violette, A., Goddéris, Y., Maréchal, J.C., Riotte, J., Oliva, P., Kumar, M.S.M., Sekhar, M., Braun, J.J., 2010a. Modelling the chemical weathering fluxes at the watershed scale in the Tropics (Mule Hole, South India): Relative contribution of the smectite/kaolinite assemblage versus primary minerals. Chem. Geol. 277, 42–60. https://doi.org/10.1016/j.chemgeo.2010.07.009.

Violette, A., Riotte, J., Braun, J.J., Oliva, P., Marechal, J.C., Sekhar, M., Jeandel, C., Subramanian, S., Prunier, J., Barbiero, L., Dupre, B., 2010b. Formation and preservation of pedogenic carbonates in South India, links with paleo-monsoon and pedological conditions: Clues from Sr isotopes, U-Th series and REEs. Geochim. Cosmochim. Acta 74, 7059–7085. https://doi.org/10.1016/j.gca.2010.09.006.

Walthert, L., Graf, U., Kammer, A., Luster, J., Pezzotta, D., Zimmermann, S., Hagedorn, F., 2010. Determination of organic and inorganic carbon, δ13C, and nitrogen in soils containing carbonates after acid fumigation with HCl. J. Plant Nutr. Soil Sci. 173, 207–216. https://doi.org/10.1002/jpln.200900158.

Wiriyakitnateekul, W., Suddhiprakarn, A., Kheoruenromne, I., Smirk, M.N., Gilkes, R.J., 2007. Iron oxides in tropical soils on various parent materials. Clay miner. 42, 437–451. https://doi.org/10.1180/claymin.2007.042.4.02.

Yeasmin, S., Singh, B., Johnston, C.T., Sparks, D.L., 2017. Evaluation of pre-treatment procedures for improved interpretation of mid infrared spectra of soil organic matter. Geoderma 304, 83–92. https://doi.org/10.1016/j.geoderma.2016.04.008.

Yost, J.L., Hartemink, A.E., 2020. How deep is the soil studied – an analysis of four soil science journals. Plant Soil 452, 5–18. https://doi.org/10.1007/s11104-020-04550-z.

Zech, W., Schad, P., Hintermaier-Erhard, G., 2014. Böden der Welt - Ein Bildatlas, 2nd ed. Springer Spektrum, Berlin, Heidelberg. https://doi.org/10.1007/978-3-642-36575-1.